

Global database of actual nitrogen loss rates in coastal and marine sediments

Yongkai Chang¹, Ehui Tan^{1*}, Dengzhou Gao², Cheng Liu³, Zongxiao Zhang⁴,
Zhixiong Huang¹, Jianan Liu¹, Yu Han¹, Zifu Xu¹, Bin Chen⁵, Shuh-Ji Kao^{1*}

¹ State Key Laboratory of Marine Resource Utilization in South China Sea, School of
Marine Science and Engineering, Hainan University, Haikou, China

² Key Laboratory for Humid Subtropical Eco-Geographical Processes of the Ministry
of Education, School of Geographical Sciences, Fujian Normal University, Fuzhou,
China

³ Shandong Key Laboratory of Eco-Environmental Science for the Yellow River Delta,
Shandong University of Aeronautics, Binzhou, China

⁴ School of Environmental Science and Engineering, Southern University of Science
and Technology, Shenzhen, Guangdong, China

⁵ State Key Laboratory of Marine Environmental Science, College of Ocean and Earth
Sciences, Xiamen University, Xiamen, China

***Corresponding author:**

Ehui Tan (ehuitan@hainanu.edu.cn) and Shuh-Ji Kao (sjkao@hainanu.edu.cn)

Abstract

Denitrification and anaerobic ammonium oxidation (anammox) convert reactive nitrogen to inert N_2 , and play vital roles in nitrogen removal in coastal and marine ecosystems, weakening the adverse effects caused by terrestrial excessive nitrogen inputs. Given the importance of denitrification and anammox in nitrogen cycle, lots of studies have measured denitrification and anammox through intact core incubations across different systems, and nitrogen loss processes are affected by a series of environmental factors such as organic carbon, nitrate, dissolved oxygen and temperature. However, a global synthesis of actual nitrogen loss rates is lacking and how environmental factors regulate nitrogen loss remains unclear. Therefore, we have compiled a database of nitrogen loss rates, including denitrification and anammox in coastal and marine systems from published literatures. This database includes 473, 466, and 255 measurements for total nitrogen loss, denitrification and anammox, respectively. This work deepens our understanding of the spatial and temporal distribution of denitrification, anammox and the relative contribution of anammox to total nitrogen loss and their corresponding environmental controls. To our knowledge, the constructed database for the first time offers a comprehensive overview of actual nitrogen loss rates in coastal and marine ecosystems on a global scale. This database can be utilized to compare nitrogen loss rates of different regions, identify the key factors regulating these rates, and parameterize biogeochemical models in the future. This database is available in Figshare repository : <https://doi.org/10.6084/m9.figshare.27745770.v3> (Chang et al., 2024).

40 **KEYWORDS:** nitrogen cycle, denitrification, anammox, coastal and marine

41 ecosystems, isotope pairing technology, intact core incubations

42

1 Introduction

The production of anthropogenic reactive nitrogen has intensified remarkably since the mid-20th century to meet the increasing global population (Kennedy, 2021). It is estimated that nitrogen is entering Earth's ecosystems at more than twice its natural rate, drastically disrupting the pristine nitrogen cycle (Canfield et al., 2010). Much of the excess nitrogen, primarily in the form of nitrate, is conveyed downriver to coastal and marine systems due to the low use efficiency of crops (Cui et al., 2013), resulting in a series of environmental issues including harmful algal blooms, eutrophication, and hypoxia (Dai et al., 2023). Consequently, it is critical to understand the transformations, particularly the fates of reactive nitrogen, encountering the fact that the nitrogen cycle has been intensively altered and is currently functioning beyond the safe operating space for humanity (Richardson et al., 2023).

Denitrification and anammox (Anaerobic Ammonium Oxidation) are two key nitrogen loss processes in aquatic environments, playing important roles in mitigating the adverse effects of excessive nitrogen inputs (Chen et al., 2021; Tan et al., 2022).

Denitrification is the sequential reduction of nitrate, nitrite, nitric oxide, and nitrous oxide (N_2O) to dinitrogen gas (N_2), which is the most energetically favorable respiratory pathway in the absence of oxygen (Devol, 2015), serving as the predominant mechanism for nitrogen loss in coastal ecosystems (Damashek & Francis, 2018; Deng et al., 2024). Anaerobic ammonium oxidation (Anammox), an alternate nitrogen loss pathway, utilizes nitrite and ammonium to generate N_2 with no greenhouse gas N_2O production under anaerobic conditions (Graaf et al., 1995), and is

65 a chemoautotrophic process with no direct demand for organic carbon (Strous et al.,
66 1999). Therefore, anammox is an environment-friendly and energy-saving process
67 compared to denitrification.

68 The ^{15}N isotope pairing technique (IPT) has been applied to a variety of sediments to
69 quantify nitrogen loss rates in these settings (Nielsen, 1992; Robertson et al., 2019).

70 Slurry incubation and intact core incubations in combination with IPT are two widely
71 used methods for studying benthic nitrogen transformation pathways (Song et al.,

72 2016b). Slurry incubations have been used to estimate the potential rates, and have
73 advantages in discovering nitrogen loss processes in the environment (Thamdrup &
74 Dalsgaard, 2002) as well as studying the environmental controls of these pathways.

75 However, the natural gradients of substrates and redox in sediments were disrupted
76 during incubations (Trimmer et al., 2006). The intact core incubations can quantify
77 nitrogen removal processes in intact sediments and reflect the genuine benthic
78 nitrogen transformation rates. The application of intact core incubations will enable us

79 to fully clarify and understand the nitrogen cycle in field aquatic ecosystems.

80 Over the past thirty years, the introduction of isotope pairing technology has enabled
81 numerous studies to measure anammox and denitrification using intact core

82 incubations across a range of coastal and marine environments. These environments
83 include intertidal wetlands (Adame et al., 2019; Liu et al., 2020), estuaries and coasts
84 (Chen et al., 2021; Cheung et al., 2024; Deek et al., 2013; Helleman et al., 2017),

85 lagoons (Bernard et al., 2015; Magri et al., 2020) and oceans (Deutsch et al., 2010; Na
86 et al., 2018). Despite decades of observations, the majority of studies on

删除[小子]: due to advantage of simple operation in incubations (Thamdrup & Dalsgaard, 2002),

删除[小子]: a large number of studies have used this method to study sediment

设置格式[小子]: 字体: (默认) Times New Roman, (中文) 宋体, 小四

删除[小子]: .

删除[小子]: H

删除[小子]: slurry incubations could not reflect the genuine benthic nitrogen transformation rates, as

删除[小子]: application of

设置格式[小子]: 字体: (默认) Times New Roman, (中文) 宋体, 小四

删除[小子]: overcome this drawback and

删除[小子]: research

87 denitrification and anammox have been limited to local or regional scales. Various
88 environmental factors, such as the availability of organic carbon (Yin et al., 2015) and
89 nitrate (Asmala et al., 2017), dissolved oxygen (Bonaglia et al., 2013; Song et al.,
90 2021), and temperature (Tan et al., 2022) influence these processes in coastal marine
91 ecosystems. The modeling community also has conducted many researches on
92 environmental regulation of nitrogen loss (mainly denitrification), and improved the
93 predictive parameters of denitrification (Middelburg et al., 1996; Bohlen et al., 2012;
94 Li et al., 2024). However, according to the currently available observational data, the
95 global patterns and drivers of sediment nitrogen loss rates remain poorly understood
96 in coastal and marine systems.

97 In view of the critical role of nitrogen removal processes and the current lack of a
98 comprehensive database on actual nitrogen loss in coastal and marine systems, we
99 have integrated actual nitrogen loss rates, including denitrification and anammox,
100 from published studies, and constructed a dataset on nitrogen removal rates in these
101 systems. This study provides a global-scale overview of the biogeography and
102 potential controlling factors of denitrification and anammox in coastal and marine
103 ecosystems. It also highlights the potential applications of this database such as using
104 machine learning to predict the distribution of denitrification and anammox and
105 offering a crucial dataset for the parameterization and development of biogeochemical
106 models.

设置格式[小子]: 字体: (默认) Times New Roman, (中文)
宋体, 小四

设置格式[小子]: 字体: (默认) Times New Roman, (中文)
宋体, 小四

设置格式[小子]: 字体: (默认) Times New Roman, (中文)
宋体, 小四

设置格式[小子]: 字体: (默认) Times New Roman, (中文)
宋体, 小四

删除[小子]: to date

2 Methods

2.1 Data compilation

Nitrogen loss rates, including denitrification and anammox measured through intact core incubations in coastal and marine ecosystems, were extracted from the literature published between 1996 and 2024. Table 1 summarized the locations, observation numbers, core incubation methods and references of nitrogen loss rates measurements.

The intact core incubations in this study include both traditional core incubations (Bonaglia et al., 2017; Cheung et al., 2024) and continuous-flow experiments (Liu et al., 2020; McTigue et al., 2016). For continuous-flow experiments, incubations were carried out in a flow-through system where bottom water was pumped over intact cores using a multi-channel peristaltic pump, and inflow and outflow samples were collected to quantify the nitrogen process rates after the addition of ¹⁵N tracer (Gardner & McCarthy, 2009). The peer-reviewed articles compiled in this study were

sourced from the Web of Science database as of June 2024. The search terms were “denitrification” or “anammox” or “nitrogen loss” or “nitrogen removal”. Given a recent study has already summarized the data on nitrogen loss rates by slurry incubations in aquatic systems (He et al., 2025), this work only selected data in which denitrification and/or anammox rates were measured using intact core incubations with ¹⁵N isotope pairing techniques, excluding measurements derived from slurry incubations. The intact core incubation experiments were primarily conducted in dark conditions and near-*in situ* or *in situ* ambient temperatures. Photosynthetic O₂

删除[小子]:
删除[小子]: combined with core incubations

设置格式[小子]: 上标

删除[小子]: O
删除[小子]: where
删除[小子]: combined
删除[小子]: were included
删除[小子]: while those measured via slurry incubation were excluded
设置格式[小子]: 下标

128 production can influence O₂ penetration depth and thereby nitrate availability in
129 sediments, interfering with denitrification rates in the nitrate reduction zone (Chen et
130 al., 2021; Bartoli et al., 2021). In cases where nitrogen loss rates were measured under
131 both light and dark conditions, only those measured in the dark were included to
132 avoid photosynthesis and facilitate comparison with other studies. Measurements
133 under light conditions have been detailed in studies reported by Bartoli et al. (2021),
134 Chen et al. (2021), Risgaard-Petersen et al. (2004), Rysgaard et al. (1996b), and Welsh
135 et al. (2000). Some studies have investigated the changes in nitrogen loss processes
136 under varying oxygen concentrations (Bonaglia et al., 2013; Neubacher et al., 2011;
137 Song et al., 2021), however, only nitrogen loss rates measured under ambient oxygen
138 concentrations were extracted for this database. Some coastal zones are inhabited by
139 plants and animals, whole core incubation would exclude the effect of benthic fauna
140 or bioturbation as the nutrient and oxygen availabilities in the core might not reflect *in*
141 *situ* sediment characteristics. In addition, whole core incubation would exclude the
142 effect of antibiotics addition because antibiotics addition could influence *in situ*
143 nitrogen removal rates (Wan et al., 2023). Thus, studies examining the effects of
144 meiofauna or antibiotics on nitrogen removal were not included (Bonaglia et al.,
145 2014b; Wan et al., 2023), only rates measured without meiofauna or antibiotic
146 additions were considered. At least one environmental variable was recorded for each
147 selected study, and means and sample sizes had to be reported for nitrogen removal
148 rates. Articles that only reported nitrogen loss rates without any environmental
149 variables were excluded. Data on total nitrogen loss rates (the sum of denitrification

设置格式[小子]: 下标

设置格式[小子]: 字体: (默认) Times New Roman, (中文) 宋体, 小四, 字体颜色: 自动设置, 非突出显示

设置格式[小子]: 字体: 倾斜

设置格式[小子]: 字体: 倾斜

删除[小子]: Additionally, studies examining the effects of meiofauna or antibiotics on nitrogen removal

删除[小子]: were not included

and anammox), denitrification rates, anammox rates, and related environmental variables were collected from tables, text, and/or supplementary materials, and in some cases, extracted from graphs using Origin 2020 software. The unit conversions were performed where necessary. For example, nitrogen loss (including denitrification and anammox) rates were in $\mu\text{mol N m}^{-2} \text{ h}^{-1}$. When rates in the texts were displayed as $\text{mmol N m}^{-2} \text{ d}^{-1}$ or $\mu\text{mol N m}^{-2} \text{ d}^{-1}$, they were converted to $\mu\text{mol N m}^{-2} \text{ h}^{-1}$. In addition, longitude and latitude were extracted from figures from published articles if not shown in the main text.

The database includes observation details (year of sampling, month of sampling, latitude, and longitude), sediment parameters, and water physicochemical factors, such as sediment organic carbon, the ratios of carbon to nitrogen (C/N ratios), oxygen penetration depth, and water salinity, depth, temperature, DO, ammonium and nitrate concentrations. Note that some environmental variables were not reported in the original studies. NM represents parameters that were not measured, and empty or NA indicates data not available or reported. In total, the database comprises 473, 466, 255, and 255 measurements of total nitrogen loss rates, denitrification rates, anammox rates, and the relative contribution of anammox to total nitrogen loss, respectively. Authors and interested readers are welcomed to contact us to indicate an error or update the data in the database.

For quality control, extreme nitrogen loss rate values were excluded from the database following Chauvenet's criterion (Glover et al., 2011), a method typically applied to

172 normally distributed data to identify outliers whose deviation from the mean has a
173 probability lower than $1/(2n)$. More details about Chauvenet's criterion can be found
174 in Glover et al., (2011) and Buitenhuis et al. (2013). Very high rates of denitrification
175 were observed in the Tama Estuary, Japan (Usui et al., 2001), a constructed wetland in
176 Casino, NSW, Australia (Erler et al., 2008), a coastal lagoon in Sacca di Goro lagoon,
177 Italy (Magri et al., 2020) and the Tropical Coastal Wetlands, Australia (Adame et al.,
178 2019). For anammox, high rates were found only in a constructed wetland in Casino,
179 NSW, Australia (Erler et al., 2008). Similarly, high values for anammox's contribution
180 to total nitrogen loss were observed in the Changjiang River Estuary (also called
181 Yangtze River Estuary), China (Liu et al., 2020), the Norwegian Trench, Skagerrak
182 (Trimmer et al., 2013), and the Great Barrier Reef lagoon (Erler et al., 2013), with
183 contributions exceeding 70%. Observations with nitrogen loss rates of 0 or NA were
184 excluded from the outlier analysis. For example, anammox rates of 0 were reported in
185 the Changjiang River Estuary, China (Liu et al., 2020), the North Sea (Neubacher et
186 al., 2011; Rosales Villa et al., 2019), the Pearl River Estuary, China (Tan et al., 2019),
187 the Norwegian Trench, Skagerrak (Trimmer et al., 2013), and the Gulf of Finland,
188 Baltic Sea (Jäntti et al., 2011). After excluding observations of 0 and NA (0, 8, 252,
189 and 253 observations for total nitrogen loss rates, denitrification rates, anammox rates,
190 and anammox's contribution to total nitrogen loss), the nitrogen loss rates were
191 natural-log transformed for further analysis.

设置格式[小子]: 字体: (默认) Times New Roman, 小四

设置格式[小子]: 字体: (默认) Times New Roman, 小四

2.2 Methods for measuring denitrification and anammox rates

Before the discovery of anammox, denitrification was regarded as the sole significant pathway responsible for nitrogen loss (Dalsgaard & Thamdrup, 2002). The ^{15}N isotope pairing technique (IPT) was developed to quantify denitrification rates (Nielsen, 1992). In this method, the overlying water of intact sediment cores is enriched with $^{15}\text{NO}_3^-$, which is mixed with the naturally occurring $^{14}\text{NO}_3^-$. After a few hours of incubation, the denitrification products, ^{15}N -labeled dinitrogen gas ($^{29}\text{N}_2$ and $^{30}\text{N}_2$), are measured. Incubations to measure nitrogen loss rates have been mostly conducted in dark conditions and near-*in situ* or *in situ* ambient temperatures. After incubating for 1 h to over 96 h, the incubation is halted by injecting saturated HgCl_2 or ZnCl_2 saturation solution or 37% formaldehyde. The samples are then preserved for $^{15}\text{N}_2$ gas analyses through isotope ratio mass spectrometer (IRMS) or membrane inlet mass spectrometry (MIMS). Key experimental details, such as incubation conditions, temperature control, incubation time, termination, and calculation references, are compiled in the database if provided in the original studies. For more detailed experimental information, refer to the corresponding references.

The production rate of unlabeled $^{14}\text{NO}_3^-$ (IPT_{p14}, also referred to as the genuine production of N_2) can be calculated based on the assumption of random isotope pairing during the denitrification of the uniformly mixed NO_3^- species. The following equation is commonly used to estimate the genuine N_2 production (Nielsen, 1992; Steingruber et al., 2001).

$$\text{IPT}p14 = \frac{p^{29}\text{N}_2}{2 \times p^{30}\text{N}_2} \times (p^{29}\text{N}_2 + 2 \times p^{30}\text{N}_2) \quad (1)$$

Where $p^{29}\text{N}_2$ and $p^{30}\text{N}_2$ represent the total production rates of $^{29}\text{N}_2$ and $p^{30}\text{N}_2$, respectively.

Thamdrup and Dalsgaard (2002) were the first to quantify anammox through anaerobic slurry incubations in natural environments, discovering that anammox could account for more than 60% of total N_2 production. This highlighted the significant role of anammox in nitrogen removal. Following this, Risgaard-Petersen et al. (2003) proposed a modification to the traditional IPT, allowing for more accurate quantification of true N_2 production in environments where anammox and denitrification coexist. This revision also enables the distinction between N_2 produced by anammox and denitrification. The revised IPT (rIPT) follows the same procedure as the classical IPT, with $^{15}\text{NO}_3^-$ added to the overlying water of intact sediment cores, though the calculation process is more complex. The following equations are commonly used to estimate the actual N_2 production (rIPT $p14$) and denitrification ($p14\text{DEN}$) as well as anammox ($p14\text{ANA}$) (Risgaard-Petersen et al., 2003; Trimmer & Nicholls, 2009; Trimmer et al., 2006). The total N_2 production rate is the sum of denitrification and anammox rates.

$$\text{rIPT}p14 = 2r_{14} \times (p^{29}\text{N}_2 + p^{30}\text{N}_2 \times (1 - r_{14})) \quad (2)$$

$$p14\text{DEN} = 2r_{14} \times (r_{14} + 1) \times p^{30}\text{N}_2 \quad (3)$$

$$p14\text{ANA} = 2r_{14} \times (p^{29}\text{N}_2 - 2 \times r_{14} \times p^{30}\text{N}_2) \quad (4)$$

In these equations, $p^{29}\text{N}_2$ and $p^{30}\text{N}_2$ are the total production rates of $^{29}\text{N}_2$ and $p^{30}\text{N}_2$, respectively, and r_{14} represents the ratio of $^{14}\text{NO}_3^-$ and $^{15}\text{NO}_3^-$ in the nitrate reduction

zone. There are 3 different methods to estimate r_{14} , with detailed explanations available in Trimmer et al. (2006).

Subsequently, Hsu and Kao (2013) revised the rIPT method to incorporate both N_2O production and anammox, enabling the determination of the absolute rate of each nitrogen loss pathway, including denitrification, anammox, and N_2O production from denitrification. Denitrification and anammox measurements based on the method of Hsu and Kao (2013) are included in this database, whereas data on the true N_2O production rate have not been included.

Regarding the aforementioned calculation methods, Salk et al. (2017) have systematically reviewed different methods for quantifying nitrogen loss rates and illustrated their differences with diagrams distinguishing different processes, providing valuable guidance for researchers interested in this field. Therefore, interested researchers can refer to their article.

删除[小子]: s

设置格式[小子]: 字体: (默认)Times New Roman, 小四, 非突出显示

3 Results and discussion

3.1 Overview of the database

Overall, there are 473, 466, and 255 measurements for total nitrogen loss denitrification and anammox, respectively (Fig. 1). Denitrification and anammox have been measured simultaneously at 255 observations. The observations of nitrogen loss rates are primarily distributed in the Eastern coast of the United States, the Baltic Sea, the Eastern Coast of China, the Eastern Coast of Australia, and polar regions of the Northern Hemisphere (Fig. 1a). Before 2000, nitrogen loss measurements were

256 predominantly focused on denitrification, while both denitrification and anammox
257 rates have been measured concurrently since 2000 (Fig. 1b). Notably, more
258 observations were recorded in 2011 and 2017. The studies in 2011 were mainly
259 conducted in the Changjiang estuary and its adjacent East China Sea (Song et al.,
260 2021), the Jinpu Bay, China (Yin et al., 2015), the North Sea (Bale et al., 2014), the
261 Northern Baltic Proper (Bonaglia et al., 2014a) and the hypoxic zone off the
262 Changjiang River estuary, China (Yang et al., 2022). In 2017, high observations were
263 found in the Northern East China Sea, China (Chang et al., 2021), the Changjiang
264 River Estuary, China (Liu et al., 2020; Liu et al., 2019; Tan et al., 2022), the Coast of
265 Victoria, Australia (Kessler et al., 2018) and the Jiulong River Estuary, China (Tan et
266 al., 2022).

267

268 **3.2 Distribution of denitrification**

269 In total, the vast majority of nitrogen loss rate measurements were conducted in the
270 Northern Hemisphere, and data in the Southern Hemisphere were limited (Fig. 2a, 2b,
271 2c). The low and middle latitudes of the Northern Hemisphere have a large body of
272 observations, especially in the 20-30°N, 30-40°N, and 50-60°N latitude bands.
273 Denitrification rates ranged from 0.04 to 750 $\mu\text{mol N m}^{-2} \text{ h}^{-1}$, with a median value of
274 $7.72 \pm 4.30 \mu\text{mol N m}^{-2} \text{ h}^{-1}$. There is a decreasing trend in the denitrification rates with
275 latitude in the Northern Hemisphere, though the observations in the high latitude are
276 still limited. The measurements of denitrification were primarily conducted between

删除[小子]: most

删除[小子]: ly

删除[小子]: in later spring, summer, and early autumn,

删除[小子]: from

277 April ~~and~~ September (Fig. 2d, 2e, 2f). On a global scale, no clear seasonal pattern for
278 denitrification rates was observed.

280 **3.3 Distribution of anammox**

281 From a latitude perspective, the distribution of anammox rates closely mirrored that of
282 denitrification, with the majority of observations concentrated in the 20-30°N,
283 30-40°N, and 50-60°N latitude bands (Fig. 3a, 3b, 3c). However, compared to
284 denitrification, there were fewer anammox observations. Anammox rates spanned
285 from 0.01 to 48.94 $\mu\text{mol N m}^{-2} \text{ h}^{-1}$, with a median value of $1.00 \pm 0.39 \mu\text{mol N m}^{-2} \text{ h}^{-1}$.
286 Similar to denitrification, anammox rates also showed a decreasing trend with
287 increasing latitude in the Northern Hemisphere. Numerous anammox measurements
288 were conducted between April and September, consistent with the timing of
289 denitrification measurements (Fig. 3d, 3e, 3f). Additionally, February saw a high
290 number of anammox observations, and these observations were predominantly
291 conducted at the north East China Sea (Chang et al., 2021), the Changjiang Estuary
292 (Liu et al., 2019) and the Northeastern New Zealand continental shelf regions
293 (Cheung et al., 2024). On a global scale, there was no clear seasonal pattern for
294 anammox rates.

3.4 Distribution of contribution of anammox to total N₂ production

The relative importance of anammox to total N₂ production increased first and then decreased, peaking in the 40-50°N latitudinal band in the Northern Hemisphere, although data points in this band were limited (Fig. 4). The contribution of anammox to total N₂ production varied from 0.22% to 67.33%, with a median value of 12.29%. The highest value (67.33%) was recorded at a site on the North Atlantic continental slope at a depth of 2000 m (Trimmer & Nicholls, 2009), where anammox accounted for the majority of nitrogen removal. There were no significant monthly changes in the relative importance of anammox to total nitrogen loss, except for March, when anammox contributed a notably high percentage. High values in March were observed in the Ulleung Basin, East Sea, and the continental shelf and slope, North Atlantic (Na et al., 2018; Trimmer & Nicholls, 2009) where the stations were characterized by low nitrate levels or deep water. These environmental conditions may inhibit denitrification, thereby increasing the relative contribution of anammox to nitrogen

loss. It is worth noting that the rate observations in March were mainly distributed in certain regions. Thus, the extrapolations of relative importance of anammox in coastal marine ecosystems at the monthly level using this result should be cautious. More observation data in other regions are needed in the future.

设置格式[小子]: 字体: (默认)Times New Roman, 小四, 非突出显示

设置格式[小子]: 字体: (默认)Times New Roman, 小四, 非突出显示

设置格式[小子]: 字体: (默认)Times New Roman, 小四, 非突出显示

设置格式[小子]: 字体: (默认)Times New Roman, 小四, 非突出显示

设置格式[小子]: 字体: (默认)Times New Roman, 小四, 非突出显示

3.5 Control factors on denitrification and anammox rates

删除[小子]: nitrogen loss

The variations in denitrification rates, and anammox rates, were compared against several environmental variables, including sediment organic carbon, the ratios of carbon to nitrogen (C/N ratios) and oxygen penetration depth, and water depth, temperature, salinity, dissolved oxygen, ammonium, and nitrate concentrations. This comparison was conducted to evaluate the main controlling factors of nitrogen loss rates.

删除[小子]: ,

删除[小子]: , and the contribution of anammox to total N₂ production (%)

There was no significant relationship between denitrification rates and the contents of sediment organic carbon ($p>0.05$; Fig. 5a). Heterotrophic denitrification is primarily carried out by facultative anaerobic heterotrophs (Devol, 2015), which use organic carbon as an electron donor and energy source. Therefore, higher organic carbon levels might be expected to promote denitrification (Damashek & Francis, 2018). However, no such relationship was observed in this dataset. Denitrification rates increased with sediment carbon nitrogen ratios ($r=0.32$, $p<0.01$; Fig. 5b). The C/N ratios can indicate the reactivity of sediment organic material, with lower C/N values generally representing more reactive organic matter (Cheung et al., 2024; Erler et al., 2013). Typically, high denitrification rates are associated with sediments that have lower C/N ratios. However, in this analysis, the opposite trend was observed. One possible explanation is that microbial communities may adapt to use organic matter typically encountered, though the organic matter is not labile (Salk et al., 2017). Denitrification rates showed a weak negative correlation with oxygen penetration depth ($r=-0.29$, $p<0.01$; Fig. 5c), as greater O₂ penetration may be adverse to the

删除[小子]: and the relative importance of anammox to total nitrogen removal

删除[小子]: 2

occurrence of denitrification (Cheung et al., 2024). Denitrification rates also decreased with water depth ($r=-0.26$, $p<0.01$; Fig. 5d), with most observations occurring at depths shallower than 250 m. Denitrification was positively correlated with higher water temperatures ($r=0.38$, $p<0.01$; Fig. 5e), and negatively correlated with salinity ($r=-0.15$, $p<0.01$; Fig. 5f), with most rates falling within two salinity ranges (0-10 and 30-40). Samples that had a salinity greater than 40 were collected in hypersaline lagoons of tropical regions (Enrich-Prast et al., 2016). The relationship between denitrification and salinity across coastal environments has been summarized by Torregrosa-Crespo et al. (2023) and will not be further elaborated here. There was a weak negative relationship between denitrification rates and dissolved oxygen concentrations ($r=-0.23$, $p<0.01$; Fig. 5g). Overall, higher denitrification rates were recorded in areas with high nitrate concentrations ($r=0.16$, $p<0.01$; Fig. 5h), suggesting the importance of nitrate substrate in regulating denitrification, though some high rates were also observed in sites with low nitrate levels. No significant correlation was found between denitrification rates and ammonium concentrations ($p>0.05$; Fig. 5i).

Anammox rates showed a weak positive correlation with sediment organic carbon ($r=0.16$, $p<0.05$; Fig. 6a). Although anammox is an autotrophic process that does not require organic carbon as an electron donor (Salk et al., 2017), some studies have reported links between sediment organic carbon content and anammox rates. For example, studies in subtropical mangrove sediments (Meyer et al., 2005) and the

360 Thames estuary (Trimmer et al., 2003) found that higher organic matter stimulated
361 anammox. This correlation may be due to enhanced mineralization leading to
362 increased ammonium production, which indirectly stimulates anammox (Damashek &
363 Francis, 2018), as sediment organic carbon can serve as a proxy for organic carbon
364 mineralization (Song et al., 2016a). Similar to denitrification, high anammox rates
365 were observed at sites with elevated C/N ratios ($r=0.33$, $p<0.01$; Fig. 6b). We infer
366 that, to some extent, the coupling of denitrification and anammox may account for
367 this relation. As mentioned above, denitrification stimulated with higher C/N ratios,
368 decomposition of organic matter could provide substrate for anammox, thereby
369 promoting anammox. More studies are needed to reveal the influencing mechanisms
370 of C/N ratios on anammox. No clear trend was found between anammox rates and
371 oxygen penetration depth ($p>0.05$; Fig. 6c), and high anammox rates were observed in
372 shallow waters ($p>0.05$; Fig. 6d). Anammox rates showed a weak positive correlation
373 with temperature ($r=0.19$, $p<0.01$; Fig. 6e). While several studies have suggested that
374 low temperatures could favor anammox (Dalsgaard & Thamdrup, 2002; Rysgaard et
375 al., 2004; Tan et al., 2020), these studies primarily measured anammox potential using
376 anaerobic slurry incubations. Contrary to previous findings, our study showed that
377 actual anammox rates increased with rising temperatures, suggesting a discrepancy
378 between the effects of temperature on actual and potential anammox rates. Future
379 research is needed to investigate the underlying mechanisms for these inconsistent
380 results. Anammox rates decreased with increasing salinity ($r=-0.38$, $p<0.01$; Fig. 6f),
381 and showed no significant relationship with dissolved oxygen ($p>0.05$; Fig. 6g). A

设置格式[小子]: 字体: (默认) Times New Roman, 小四

删除[小子]: research is

删除[小子]: organic matter quantity and quality

weak positive correlation was observed between anammox rates and nitrate concentration ($r=0.41$, $p<0.01$; Fig. 6h), highlighting the importance of substrates in regulating anammox. Although anammox uses nitrite as an electron acceptor rather than nitrate (Graaf et al., 1995), nitrate reduction can produce nitrite, which promotes anammox activity. No relationship was found between anammox rates and ammonium concentration ($p>0.05$; Fig. 6i).

Through the correlation analysis of global-scale compiled data, we identified that sediment C/N ratios, oxygen penetration depth, water depth, temperature, salinity, dissolved oxygen, and nitrate concentrations were the main factors regulating denitrification rates, whereas sediment organic carbon, C/N ratios, temperature, salinity, and nitrate concentrations primarily controlled anammox rates (Fig. 5 and Fig. 6).

Other factors, such as iron, manganese, and sulfide, although not included in the database, can also influence denitrification and anammox rates. For example, Fe oxides were observed to be positively correlated with denitrification rates in the Jinpu Bay, China (Yin et al., 2015). The mechanism may be that ferrous iron can supply an electron donor for nitrate, thereby promoting denitrification. Anschutz et al. (2000) found manganese dioxides could also serve as electron donors for denitrification. Deng et al. (2015) showed a positive relationship between denitrification rates and sulfide concentrations in the Changjiang Estuary sediments, revealing that sulfide can act as energy sources for denitrification. In contrast, evidence has shown that sulfide exerts inhibitory effects on nitrogen removal in coastal sediments by inhibiting the

设置格式[小子]: 字体: (默认) Times New Roman, 小四

metabolism of denitrifying microorganisms (Aelion and Warttinger, 2010). Thus, the impact of sulfide on denitrification remains controversial. For anammox, a study found that sulfide could affect anammox activity. Yin et al. (2015) found that anammox rates were positively correlated with sulfide concentrations. This phenomenon is likely attributed to sulfide-induced nitrite accumulation during incomplete denitrification processes, where sulfide inhibits the activity of nitric oxide reductase and nitrous oxide reductase, thereby enhancing anammox activity. Under anaerobic conditions, ammonium oxidation can be coupled with the reduction of ferric iron, sulfate, and Mn(IV)-oxides. For example, Rios-Del Toro et al. (2018) confirmed that ammonium oxidation was associated with ferric iron and sulfate reduction under anaerobic conditions, thereby stimulating nitrogen loss in marine sediments. Evidence shows ammonium loss is coupled with Fe(III) and Mn(IV) reduction in coastal environments (Samperio-Ramos et al., 2024), demonstrating the crucial roles of metal oxides in removing reactive nitrogen.

Liu et al. (2020) have examined the spatio-temporal changes of *in situ* nitrogen loss processes in intertidal wetlands of the Yangtze Estuary and found that denitrification was linked to anammox, implying the coupling of denitrification and anammox on a local scale. Consistent with their findings, this work also found denitrification was positively correlated to anammox ($r=0.67$, $p<0.01$; Fig. 7). A majority of denitrifying bacteria are heterotrophic, and the decomposition of organic matter is accompanied by the production of ammonium (Devol, 2015), supplying substrates for anammox. Thus,

删除[小子]: Numerous studies

设置格式[小子]: 字体: 倾斜

设置格式[小子]: 字体: (默认) Times New Roman, (中文) 宋体, 小四, 倾斜, 无下划线, 非突出显示

设置格式[小子]: 字体: (默认) Times New Roman, (中文) 宋体, 小四, 无下划线, 非突出显示

设置格式[小子]: 字体: (默认) Times New Roman, (中文) 宋体, 小四, 无下划线, 非突出显示

设置格式[小子]: 字体: (默认) Times New Roman, (中文) 宋体, 小四, 无下划线, 非突出显示

删除[小子]: have

删除[小子]: in different habitats

删除[小子]: including estuary sediments (Liu et al., 2020), coastal wetland sediments (Gao et al., 2017) and paddy soils (Shan et al., 2016)

删除[小子]: and capable of utilizing organic matter,

the positive relationship may suggest the tight coupling of these two nitrogen removal pathways on a global scale.

3.6 Drivers on contribution of anammox to total nitrogen loss

We made simple correlation analysis between the contribution of anammox to total N_2 production (r_a) and environmental parameters (Fig. 8). There was a positive correlation between r_a and water depth ($r=0.59$, $p<0.01$; Fig. 8d). Similar findings were found on the Northeastern New Zealand continental shelf (Cheung et al., 2024) and the continental shelf and slope, North Atlantic (Trimmer & Nicholls, 2009). The increased importance of anammox can be attributed to the significant attenuation of denitrification with depth, as the availability of organic carbon, essential for heterotrophic denitrification, generally decreases with water depth (Thamdrup, 2012). In addition to water depth, other factors such as oxygen penetration depth, C/N ratios, and temperature may also influence the relative importance of anammox. The r_a was positively correlated with oxygen penetration depth ($r=0.7$, $p<0.01$; Fig. 8c). As previously mentioned, denitrification decreases with higher oxygen penetration depth, likely increasing the relative importance of anammox indirectly. Conversely, r_a showed a decreasing trend with elevated C/N ratios ($r=-0.35$, $p<0.01$; Fig. 8b). High C/N ratios may promote denitrification more significantly than anammox because both processes tend to enhance with increasing C/N ratios, leading to a decrease in the relative importance of anammox at sites with high C/N ratios. Additionally, r_a was

删除[小子]: between denitrification and anammox

删除[小子]:

设置格式[小子]: 下标

设置格式[小子]: 字体: (默认) Times New Roman, 小四

删除[小子]: the contribution of anammox to total N_2 production (

删除[小子]:)

删除[小子]: Previous studies have reported s

删除[小子]: , including those conducted

删除[小子]: ,

删除[小子]: , which is

删除[小子]: ,

删除[小子]: increasing

删除[小子]: contribution of anammox to total N_2 production (

删除[小子]:)

negatively correlated with temperature ($r=-0.29$, $p<0.01$; Fig. 8e), indicating that denitrification is stimulated at higher temperatures compared to anammox. Temperature-controlled experiments have confirmed that denitrification has a greater optimal temperature than anammox (Canion et al., 2014; Tan et al., 2020). No correlations were found between r_a and other environmental factors, including sediment organic carbon, water salinity, dissolved oxygen, nitrate, and ammonium concentrations. (all $p>0.05$; Fig. 8a, 8f, 8g, 8h, 8i). Based on the simple correlation analysis of global-scale compiled data, we identified that sediment C/N ratios, oxygen penetration depth, water depth and temperature were the primary factors governing the relative contribution of anammox to total nitrogen loss (Fig. 8).

4 Applications of the database

This database serves as a valuable resource for the broad scientific communities that are interested in nitrogen cycle processes within coastal and marine ecosystems, particularly those focusing on denitrification and anammox. The data is made accessible as a basic database that will lead to a deeper understanding and generate new scientific insights into the nitrogen cycles at the global scale. Potential applications of this database include: (1) serving as a reference for comparing denitrification and anammox rates across different spatial scales including local, regional, and global scales or across different habitats such as coastal wetland, estuary, lagoon, and ocean in future studies, (2) identifying and comparing the controlling

删除[小子]: ;

468	factors of denitrification and anammox at various spatial scales. <u>Note that</u>	设置格式[小子]: 字体: (默认) Times New Roman, 小四
469	<u>environmental variables have missing values, which limits our analysis of</u>	设置格式[小子]: 字体: (默认) Times New Roman, 小四
470	<u>environmental factors affecting nitrogen loss rates. For better studying the</u>	设置格式[小子]: 字体: (默认) Times New Roman, 小四
471	<u>environmental controls, these missing values can be filled using the multivariate</u>	设置格式[小子]: 字体: (默认) Times New Roman, 小四
472	<u>imputation with random forests method (Hou et al., 2021), (3) predicting the global</u>	设置格式[小子]: 字体: (默认) Times New Roman, 小四
473	biogeography of denitrification and anammox in coastal and marine systems through	删除[小子]: ;
474	machine learning <u>methods. For example, by integrating potential key factors of</u>	设置格式[小子]: 字体: (默认) Times New Roman, 小四
475	<u>nitrogen removal processes into machine learning architectures, future studies can</u>	设置格式[小子]: 字体: (默认) Times New Roman, 小四
476	<u>develop spatially predictive models for global nitrogen loss rates by the references of</u>	设置格式[小子]: 字体: (默认) Times New Roman, 小四
477	<u>Laffitte et al. (2025) and Ling et al. (2025), (4) providing essential data for the</u>	设置格式[小子]: 字体: (默认) Times New Roman, 小四
478	parameterization, validation and enhancement of Earth system biogeochemical	设置格式[小子]: 字体: (默认) Times New Roman, 小四
479	models. <u>The previous model considered constraint parameters such as nitrate,</u>	删除[小子]: ; and
480	<u>dissolved oxygen, chlorophyll, and phosphate content (Middelburg et al., 1996;</u>	设置格式[小子]: 字体: (默认) Times New Roman, 小四
481	<u>Bohlen et al., 2012; Li et al., 2024), and other parameters provided in this dataset can</u>	设置格式[小子]: 字体: (默认) Times New Roman, 小四
482	<u>supply new parameter supplements for the development of biogeochemical model. (5)</u>	设置格式[小子]: 字体: (默认) Times New Roman, 小四
483	<u>guiding future observations. More studies are needed in areas and months with limited</u>	设置格式[小子]: 字体: (默认) Times New Roman, 小四
484	<u>observation data on nitrogen loss rates to deepen our understanding of the nitrogen</u>	设置格式[小子]: 字体: (默认) Times New Roman, 小四
485	<u>cycle worldwide. Additionally, when studying nitrogen loss rates, particular attention</u>	设置格式[小子]: 字体: (默认) Times New Roman, 小四
486	<u>should be paid to enhancing the monitoring of multiple environmental parameters.</u>	设置格式[小子]: 字体: (默认) Times New Roman, 小四
487		设置格式[小子]: 字体: (默认) Times New Roman, 小四
		设置格式[小子]: 字体: (默认) Times New Roman, 小四
		设置格式[小子]: 字体: (默认) Times New Roman, 小四
		设置格式[小子]: 字体: (默认) Times New Roman, 小四

5 Conclusions

We compiled and presented a global database of denitrification and anammox measurements obtained from core incubation experiments in coastal and marine sediments. To our knowledge, no efforts have been made to compile actual nitrogen loss rates and associated environmental factors in coastal and marine regions on a global scale. This database offers valuable insights into the spatiotemporal variations and potential controlling factors of denitrification and anammox, along with the contribution of anammox to total N₂ production. The establishment of this global database on denitrification and anammox in coastal and marine sediments provides a critical foundation for advancing nitrogen cycle research and generating novel insights. This database enables the comparison of these two nitrogen loss processes, evaluation of the environmental controls across spatial scales (local to global), prediction of the global biogeography of denitrification and anammox, parameterization and development of biogeochemical models, and guide direction of observations in the future.

Data availability

The data used in this study are openly available in Figshare repository at <https://doi.org/10.6084/m9.figshare.27745770.v3> (Chang et al., 2024).

Author contributions

SJK and EHT conceived the research. YKC and EHT compiled the data. YKC, EHT,

设置格式[小子]: 字体: (默认) Times New Roman, 小四
删除[小子]: It can be used
删除[小子]: to
删除[小子]: e
删除[小子]:
删除[小子]: assess
删除[小子]:
删除[小子]: on them
设置格式[小子]: 字体: (默认) Times New Roman, 小四
设置格式[小子]: 字体: (默认) Times New Roman, 小四
设置格式[小子]: 字体: (默认) Times New Roman, 小四
删除[小子]: at regional and global levels
删除[小子]:
设置格式[小子]: 字体: (默认) Times New Roman, 小四
设置格式[小子]: 字体: (默认) Times New Roman, 小四
删除[小子]: and support the
删除[小子]: ment of

DZG, CL and SJK participated in the data analysis. All co-authors contributed to the writing and reviewing of this manuscript.

Competing interests

None declared.

Acknowledgements

We thank the authors for their contributions to the data used in this database. Thanks to the editors and reviewers for their constructive comments and suggestions that improved this manuscript greatly.

Financial support

This work was supported by the National Natural Science Foundation of China (92251306 and 42276043), the Hainan Provincial Natural Science Foundation of China (623RC456), the Collaborative Innovation Center of Marine Science and Technology in Hainan University (XTCX2022HYC19), the Innovative Fund for Scientific and Technological Personnel of Hainan Province (KJRC2023B04) and the Shandong Provincial Natural Science Foundation of China (ZR2023QD103).

References

Adame, M. F., Roberts, M. E., Hamilton, D. P., Ndehedehe, C. E., Reis, V., Lu, J., Griffiths, M., Curwen, G., and Ronan, M.: Tropical Coastal Wetlands Ameliorate Nitrogen Export During Floods, *Front. Mar. Sci.*, 6, <https://doi.org/10.3389/fmars.2019.00671>, 2019.

Aelion, C. M. and Warttinger, U.: Sulfide Inhibition of Nitrate Removal in Coastal Sediments, Estuaries Coasts, 33, 798-803, <https://doi.org/10.1007/s12237-010-9275-4>, 2010.

Anschutz, P., Sundby, B., Lefrançois, L., Luther, G. W., and Mucci, A.: Interactions between metal oxides and species of nitrogen and iodine in bioturbated marine sediments, Geochim. Cosmochim. Acta, 64, 2751-2763, [https://doi.org/10.1016/S0016-7037\(00\)00400-2](https://doi.org/10.1016/S0016-7037(00)00400-2), 2000.

Arroyave Gómez, D. M., Gallego Suárez, D., Bartoli, M., and Toro-Botero, M.: Spatial and seasonal variability of sedimentary features and nitrogen benthic metabolism in a tropical coastal area (Taganga Bay, Colombia Caribbean) impacted by a sewage outfall, Biogeochemistry, 150, 85-107, <https://doi.org/10.1007/s10533-020-00689-0>, 2020.

Asmala, E., Carstensen, J., Conley, D. J., Slomp, C. P., Stadmark, J., and Voss, M.: Efficiency of the coastal filter: Nitrogen and phosphorus removal in the Baltic Sea, Limnol. Oceanogr., 62, S222-S238, <https://doi.org/10.1002/lno.10644>, 2017.

Bale, N. J., Villanueva, L., Fan, H., Stal, L. J., Hopmans, E. C., Schouten, S., and Sinninghe Damsté, J. S.: Occurrence and activity of anammox bacteria in surface sediments of the southern North Sea, FEMS Microbiol. Ecol., 89, 99-110, <https://doi.org/10.1111/1574-6941.12338>, 2014.

Bartoli, M., Nizzoli, D., Zilius, M., Bresciani, M., Pusceddu, A., Bianchelli, S., Sundbäck, K., Razinkovas-Baziukas, A., and Viaroli, P.: Denitrification, Nitrogen Uptake, and Organic Matter Quality Undergo Different Seasonality in Sandy and Muddy Sediments of a Turbid Estuary, Front. Microbiol., 11, <https://doi.org/10.3389/fmicb.2020.612700>, 2021.

Benelli, S., Bartoli, M., Magri, M., Brzana, R., Kendzierska, H., Styrz-Olesiak, K., and Janas, U.: Spatial and seasonal pattern of microbial nitrate reduction in coastal

554 sediments in the Vistula River plume area, Gulf of Gdańsk, Front. Mar. Sci., 11,
 555 <https://doi.org/10.3389/fmars.2024.1333707>, 2024.

556 Bernard, R. J., Mortazavi, B., and Kleinhuizen, A. A.: Dissimilatory nitrate reduction
 557 to ammonium (DNRA) seasonally dominates NO_3^- reduction pathways in an
 558 anthropogenically impacted sub-tropical coastal lagoon, Biogeochemistry, 125, 47-64,
 559 <https://doi.org/10.1007/s10533-015-0111-6>, 2015.

560 Blackburn, T. H., Hall, P. O. J., Hulth, S., and Landén, A.: Organic-N loss by efflux
 561 and burial associated with a low efflux of inorganic N and with nitrate assimilation in
 562 Arctic sediments (Svalbard, Norway), Mar. Ecol.: Prog. Ser., 141, 283-293,
 563 <https://doi.org/10.3354/meps141283>, 1996.

564 [Bohlen, L., Dale, A. W., and Wallmann, K.: Simple transfer functions for calculating](#)
 565 [benthic fixed nitrogen losses and C:N:P regeneration ratios in global biogeochemical](#)
 566 [models, Global Biogeochem. Cycles, 26, https://doi.org/10.1029/2011GB004198,](#)
 567 [2012.](#)

568 Bonaglia, S., Deutsch, B., Bartoli, M., Marchant, H. K., and Brüchert, V.: Seasonal
 569 oxygen, nitrogen and phosphorus benthic cycling along an impacted Baltic Sea
 570 estuary: regulation and spatial patterns, Biogeochemistry, 119, 139-160,
 571 <https://doi.org/10.1007/s10533-014-9953-6>, 2014a.

572 Bonaglia, S., Nascimento, F. J. A., Bartoli, M., Klawonn, I., and Brüchert, V.:
 573 Meiofauna increases bacterial denitrification in marine sediments, Nat. Commun., 5,
 574 5133, <https://doi.org/10.1038/ncomms6133>, 2014b.

575 Bonaglia, S., Bartoli, M., Gunnarsson, J. S., Rahm, L., Raymond, C., Svensson, O.,
 576 Shakeri Yekta, S., and Brüchert, V.: Effect of reoxygenation and Marenzelleria spp.
 577 bioturbation on Baltic Sea sediment metabolism, Mar. Ecol.: Prog. Ser., 482, 43-55,
 578 <https://doi.org/10.3354/meps10232>, 2013.

579 Bonaglia, S., Hylén, A., Rattray, J. E., Kononets, M. Y., Ekeröth, N., Roos, P.,
 580 Thamdrup, B., Brüchert, V., and Hall, P. O. J.: The fate of fixed nitrogen in marine
 581 sediments with low organic loading: an in situ study, *Biogeosciences*, 14, 285-300,
 582 <https://doi.org/10.5194/bg-14-285-2017>, 2017.

583 Buitenhuis, E. T., Vogt, M., Moriarty, R., Bednaršek, N., Doney, S. C., Leblanc, K.,
 584 Le Quéré, C., Luo, Y. W., O'Brien, C., O'Brien, T., Peloquin, J., Schiebel, R., and
 585 Swan, C.: MAREDAT: towards a world atlas of MARine Ecosystem DATA, *Earth*
 586 *Syst. Sci. Data*, 5, 227-239, <https://doi.org/10.5194/essd-5-227-2013>, 2013.

587 Canfield, D. E., Glazer, A. N., and Falkowski, P. G.: The Evolution and Future of
 588 Earth's Nitrogen Cycle, *Science*, 330, 192-196,
 589 <https://doi.org/10.1126/science.1186120>, 2010.

590 Canion, A., Kostka, J. E., Gihring, T. M., Huettel, M., van Beusekom, J. E. E., Gao,
 591 H., Lavik, G., and Kuypers, M. M. M.: Temperature response of denitrification and
 592 anammox reveals the adaptation of microbial communities to in situ temperatures in
 593 permeable marine sediments that span 50° in latitude, *Biogeosciences*, 11, 309-320,
 594 <https://doi.org/10.5194/bg-11-309-2014>, 2014.

595 Chang, Y., Tan, E., Gao, D., Liu, C., Zhang, Z., Huang, Z., Liu, J., Han, Y., Xu, Z.,
 596 Chen, B., Kao, S.-J.: Global database of actual nitrogen loss rates in coastal and
 597 marine sediments, Figshare, <https://doi.org/10.6084/m9.figshare.27745770.v3>, 2024.

598 Chang, Y., Yin, G., Hou, L., Liu, M., Zheng, Y., Han, P., Dong, H., Liang, X., Gao, D.,
 599 and Liu, C.: Nitrogen removal processes coupled with nitrification in coastal
 600 sediments off the north East China Sea, *J. Soils Sediments*, 21, 3289-3299,
 601 <https://doi.org/10.1007/s11368-021-02964-5>, 2021.

602 Chen, J.-J., Erler, D. V., Wells, N. S., Huang, J., Welsh, D. T., and Eyre, B. D.:
 603 Denitrification, anammox, and dissimilatory nitrate reduction to ammonium across a
 604 mosaic of estuarine benthic habitats, *Limnol. Oceanogr.*, 66, 1281-1297,

605 <https://doi.org/10.1002/lno.11681>, 2021.

606 Cheung, H. L. S., Hillman, J. R., Pilditch, C. A., Savage, C., Santos, I. R., Glud, R. N.,
607 Nascimento, F. J. A., Thrush, S. F., and Bonaglia, S.: Denitrification, anammox, and
608 DNRA in oligotrophic continental shelf sediments, *Limnol. Oceanogr.*, 69, 621-637,
609 <https://doi.org/10.1002/lno.12512>, 2024.

610 Crowe, S. A., Canfield, D. E., Mucci, A., Sundby, B., and Maranger, R.: Anammox,
611 denitrification and fixed-nitrogen removal in sediments from the Lower St. Lawrence
612 Estuary, *Biogeosciences*, 9, 4309-4321, <https://doi.org/10.5194/bg-9-4309-2012>,
613 2012.

614 Cui, S., Shi, Y., Groffman, P. M., Schlesinger, W. H., and Zhu, Y.-G.: Centennial-scale
615 analysis of the creation and fate of reactive nitrogen in China (1910–2010), *Proc. Natl.*
616 *Acad. Sci. U. S. A.*, 110, 2052-2057, <https://doi.org/10.1073/pnas.1221638110>, 2013.

617 Dai, M., Zhao, Y., Chai, F., Chen, M., Chen, N., Chen, Y., Cheng, D., Gan, J., Guan,
618 D., Hong, Y., Huang, J., Lee, Y., Leung, K. M. Y., Lim, P. E., Lin, S., Lin, X., Liu, X.,
619 Liu, Z., Luo, Y.-W., Meng, F., Sangmanee, C., Shen, Y., Uthaipan, K., Wan Talaat, W.
620 I. A., Wan, X. S., Wang, C., Wang, D., Wang, G., Wang, S., Wang, Y., Wang, Y., Wang,
621 Z., Wang, Z., Xu, Y., Yang, J.-Y. T., Yang, Y., Yasuhara, M., Yu, D., Yu, J., Yu, L.,
622 Zhang, Z., and Zhang, Z.: Persistent eutrophication and hypoxia in the coastal ocean,
623 *Cambridge Prisms: Coastal Futures*, 1, 1-28, <https://doi.org/10.1017/cft.2023.7>, 2023.

624 Dalsgaard, T. and Thamdrup, B.: Factors Controlling Anaerobic Ammonium
625 Oxidation with Nitrite in Marine Sediments, *Appl. Environ. Microbiol.*, 68,
626 3802-3808, <https://doi.org/10.1128/AEM.68.8.3802-3808.2002>, 2002.

627 Damashek, J. and Francis, C. A.: Microbial Nitrogen Cycling in Estuaries: From
628 Genes to Ecosystem Processes, *Estuaries Coasts*, 41, 626-660,
629 <https://doi.org/10.1007/s12237-017-0306-2>, 2018.

630 Deek, A., DÃ Ãhnke, K., van Beusekom, J., Meyer, S., Voss, M., and Emeis, K.: N₂
631 fluxes in sediments of the Elbe Estuary and adjacent coastal zones, *Mar. Ecol.: Prog.*
632 *Ser.*, 493, 9-21, <https://doi.org/10.3354/meps10514>, 2013.

633 Deng, D., He, G., Ding, B., Liu, W., Yang, Z., and Ma, L.: Denitrification dominates
634 dissimilatory nitrate reduction across global natural ecosystems, *Global Change Biol.*,
635 30, e17256, <https://doi.org/10.1111/gcb.17256>, 2024.

636 Deng, F., Hou, L., Liu, M., Zheng, Y., Yin, G., Li, X., Lin, X., Chen, F., Gao, J., and
637 Jiang, X.: Dissimilatory nitrate reduction processes and associated contribution to
638 nitrogen removal in sediments of the Yangtze Estuary, *J. Geophys. Res.:Biogeosci.*,
639 120, 1521-1531, <https://doi.org/10.1002/2015JG003007>, 2015.

640 Deutsch, B., Forster, S., Wilhelm, M., Dippner, J. W., and Voss, M.: Denitrification in
641 sediments as a major nitrogen sink in the Baltic Sea: an extrapolation using sediment
642 characteristics, *Biogeosciences*, 7, 3259-3271,
643 <https://doi.org/10.5194/bg-7-3259-2010>, 2010.

644 Devol, A. H.: Denitrification, Anammox, and N₂ Production in Marine Sediments,
645 *Annu. Rev. Mar. Sci.*, 7, 403-423,
646 <https://doi.org/10.1146/annurev-marine-010213-135040>, 2015.

647 Enrich-Prast, A., Figueiredo, V., Esteves, F. d. A., and Nielsen, L. P.: Controls of
648 Sediment Nitrogen Dynamics in Tropical Coastal Lagoons, *PloS one*, 11, e0155586,
649 <https://doi.org/10.1371/journal.pone.0155586>, 2016.

650 Erler, D. V., Eyre, B. D., and Davison, L.: The Contribution of Anammox and
651 Denitrification to Sediment N₂ Production in a Surface Flow Constructed Wetland,
652 *Environ. Sci. Technol.*, 42, 9144-9150, <https://doi.org/10.1021/es801175t>, 2008.

653 Erler, D. V., Trott, L. A., Alongi, D. M., and Eyre, B. D.: Denitrification, anammox
654 and nitrate reduction in sediments of the southern Great Barrier Reef lagoon, *Mar.*

655 Ecol.: Prog. Ser., 478, 57-70, <https://doi.org/10.3354/meps10040>, 2013.

656 Erler, D. V., Welsh, D. T., Bennet, W. W., Meziane, T., Hubas, C., Nizzoli, D., and
 657 Ferguson, A. J. P.: The impact of suspended oyster farming on nitrogen cycling and
 658 nitrous oxide production in a sub-tropical Australian estuary, Estuarine, Coastal Shelf
 659 Sci., 192, 117-127, <https://doi.org/10.1016/j.ecss.2017.05.007>, 2017.

660 Fan, H., Bolhuis, H., and Stal, L. J.: Drivers of the dynamics of diazotrophs and
 661 denitrifiers in North Sea bottom waters and sediments, Front. Microbiol., 6,
 662 <https://doi.org/10.3389/fmicb.2015.00738>, 2015.

663 Farías, L., Graco, M., and Ulloa, O.: Temporal variability of nitrogen cycling in
 664 continental-shelf sediments of the upwelling ecosystem off central Chile, Deep Sea
 665 Res., Part II., 51, 2491-2505, <https://doi.org/10.1016/j.dsr2.2004.07.029>, 2004.

666 Gardner, W. S. and McCarthy, M. J.: Nitrogen dynamics at the sediment–water
 667 interface in shallow, sub-tropical Florida Bay: why denitrification efficiency may
 668 decrease with increased eutrophication, Biogeochemistry, 95, 185-198,
 669 <https://doi.org/10.1007/s10533-009-9329-5>, 2009.

670 Gardner, W. S., McCarthy, M. J., An, S., Sobolev, D., Sell, K. S., and Brock, D.:
 671 Nitrogen fixation and dissimilatory nitrate reduction to ammonium (DNRA) support
 672 nitrogen dynamics in Texas estuaries, Limnol. Oceanogr., 51, 558-568,
 673 https://doi.org/10.4319/lo.2006.51.1_part_2.0558, 2006.

674 Gihring, T. M., Canion, A., Riggs, A., Huettel, M., and Kostka, J. E.: Denitrification in
 675 shallow, sublittoral Gulf of Mexico permeable sediments, Limnol. Oceanogr., 55,
 676 43-54, <https://doi.org/10.4319/lo.2010.55.1.0043>, 2010b.

677 Gihring, T. M., Lavik, G., Kuypers, M. M. M., and Kostka, J. E.: Direct determination
 678 of nitrogen cycling rates and pathways in Arctic fjord sediments (Svalbard, Norway),
 679 Limnol. Oceanogr., 55, 740-752, <https://doi.org/10.4319/lo.2010.55.2.0740>, 2010a.

删除[小子]:

Gao, D., Li, X., Lin, X., Wu, D., Jin, B., Huang, Y., Liu, M.,
 and Chen, X.: Soil dissimilatory nitrate reduction processes in
 the *Spartina alterniflora* invasion chronosequences of a coastal
 wetland of southeastern China: Dynamics and environmental
 implications, Plant Soil, 421, 383-399,
<https://doi.org/10.1007/s11104-017-3464-x>, 2017.

680 Glover, D. M., Jenkins, W. J., and Doney, S. C.: Modeling Methods for Marine
681 Science, Cambridge University Press, Cambridge,
682 <https://doi.org/10.1017/CBO9780511975721>, 2011.

683 Glud, R. N., Holby, O., Hoffmann, F., and Canfield, D. E.: Benthic mineralization and
684 exchange in Arctic sediments (Svalbard, Norway), Mar. Ecol.: Prog. Ser., 173,
685 237-251, <https://doi.org/10.3354/meps173237>, 1998.

686 Glud, R. N., Thamdrup, B., Stahl, H., Wenzhoefer, F., Glud, A., Nomaki, H., Oguri,
687 K., Revsbech, N. P., and Kitazato, H.: Nitrogen cycling in a deep ocean margin
688 sediment (Sagami Bay, Japan), Limnol. Oceanogr., 54, 723-734,
689 <https://doi.org/10.4319/lo.2009.54.3.0723>, 2009.

690 Graaf, A. A. v. d., Mulder, A., Bruijn, P. d., Jetten, M. S., Robertson, L. A., and
691 Kuenen, J. G.: Anaerobic oxidation of ammonium is a biologically mediated process,
692 Appl. Environ. Microbiol., 61, 1246-1251,
693 <https://doi.org/10.1128/aem.61.4.1246-1251.1995>, 1995.

694 [He, G., Deng, D., Delgado-Baquerizo, M., Liu, W., and Zhang, Q.: Global Relative](#)
695 [Importance of Denitrification and Anammox in Microbial Nitrogen Loss Across](#)
696 [Terrestrial and Aquatic Ecosystems, Adv. Sci., 12, 2406857,](#)
697 <https://doi.org/10.1002/advs.202406857>, 2025.

设置格式[小子]: 字体: (默认) Times New Roman, 小四

698 Hellemann, D., Tallberg, P., Aalto, S. L., Bartoli, M., and Hietanen, S.: Seasonal cycle
699 of benthic denitrification and DNRA in the aphotic coastal zone, northern Baltic Sea,
700 Mar. Ecol.: Prog. Ser., 637, 15-28, <https://doi.org/10.3354/meps13259>, 2020.

701 Hellemann, D., Tallberg, P., Bartl, I., Voss, M., and Hietanen, S.: Denitrification in an
702 oligotrophic estuary: a delayed sink for riverine nitrate, Mar. Ecol.: Prog. Ser., 583,
703 63-80, <https://doi.org/10.3354/meps12359>, 2017.

704 Hietanen, S. and Kuparinen, J.: Seasonal and short-term variation in denitrification

705 and anammox at a coastal station on the Gulf of Finland, Baltic Sea, *Hydrobiologia*,
706 596, 67-77, <https://doi.org/10.1007/s10750-007-9058-5>, 2008.

707 Hoffman, D. K., McCarthy, M. J., Newell, S. E., Gardner, W. S., Niewinski, D. N.,
708 Gao, J., and Mutchler, T. R.: Relative Contributions of DNRA and Denitrification to
709 Nitrate Reduction in *Thalassia testudinum* Seagrass Beds in Coastal Florida (USA),
710 *Estuaries Coasts*, 42, 1001-1014, <https://doi.org/10.1007/s12237-019-00540-2>, 2019.

711 Hou, E., Wen, D., Jiang, L., Luo, X., Kuang, Y., Lu, X., Chen, C., Allen, K. T., He, X.,
712 Huang, X., and Luo, Y.: Latitudinal patterns of terrestrial phosphorus limitation over
713 the globe, *Ecol. Lett.*, 24, 1420-1431, <https://doi.org/10.1111/ele.13761>, 2021.

设置格式[小子]: 字体: (默认)Times New Roman, 小四, 非
突出显示

714 Hsu, T. C. and Kao, S. J.: Technical Note: Simultaneous measurement of sedimentary
715 N₂ and N₂O production and a modified ¹⁵N isotope pairing technique, *Biogeosciences*,
716 10, 7847-7862, <https://doi.org/10.5194/bg-10-7847-2013>, 2013.

717 Jäntti, H. and Hietanen, S.: The Effects of Hypoxia on Sediment Nitrogen Cycling in
718 the Baltic Sea, *AMBIO*, 41, 161-169, <https://doi.org/10.1007/s13280-011-0233-6>,
719 2012.

720 Jäntti, H., Stange, F., Leskinen, E., and Hietanen, S.: Seasonal variation in nitrification
721 and nitrate-reduction pathways in coastal sediments in the Gulf of Finland, Baltic Sea,
722 *Aquat. Microb. Ecol.*, 63, 171-181, <https://doi.org/10.3354/ame01492>, 2011.

723 Kennedy, C. D.: Nitrogen Overload: Environmental Degradation, Ramifications, and
724 Economic Costs, *Groundwater*, 59, 161-162, <https://doi.org/10.1111/gwat.13066>,
725 2021.

726 Kessler, A. J., Roberts, K. L., Bissett, A., and Cook, P. L. M.: Biogeochemical
727 Controls on the Relative Importance of Denitrification and Dissimilatory Nitrate
728 Reduction to Ammonium in Estuaries, *Global Biogeochem. Cycles*, 32, 1045-1057,
729 <https://doi.org/10.1029/2018GB005908>, 2018.

Koop-Jakobsen, K. and Giblin, A. E.: The effect of increased nitrate loading on nitrate reduction via denitrification and DNRA in salt marsh sediments, *Limnol. Oceanogr.*, 55, 789-802, <https://doi.org/10.4319/lo.2010.55.2.0789>, 2010.

Laffitte, B., Zhou, T., Yang, Z., Ciais, P., Jian, J., Huang, N., Seyler, B. C., Pei, X., and Tang, X.: Timescale Matters: Finer Temporal Resolution Influences Driver Contributions to Global Soil Respiration, *Global Change Biol.*, 31, e70118, <https://doi.org/10.1111/gcb.70118>, 2025.

设置格式[小子]: 字体: (默认) Times New Roman, 小四

Li, N., Somes, C. J., Landolfi, A., Chien, C. T., Pahlow, M., and Oschlies, A.: Global impact of benthic denitrification on marine N₂ fixation and primary production simulated by a variable-stoichiometry Earth system model, *Biogeosciences*, 21, 4361-4380, <https://doi.org/10.5194/bg-21-4361-2024>, 2024.

设置格式[小子]: 下标

Ling, J., Dungait, J. A. J., Delgado-Baquerizo, M., Cui, Z., Zhou, R., Zhang, W., Gao, Q., Chen, Y., Yue, S., Kuzyakov, Y., Zhang, F., Chen, X., and Tian, J.: Soil organic carbon thresholds control fertilizer effects on carbon accrual in croplands worldwide, *Nat. Commun.*, 16, 3009, <https://doi.org/10.1038/s41467-025-57981-6>, 2025.

Liu, C., Hou, L., Liu, M., Zheng, Y., Yin, G., Dong, H., Liang, X., Li, X., Gao, D., and Zhang, Z.: In situ nitrogen removal processes in intertidal wetlands of the Yangtze Estuary, *J. Environ. Sci.*, 93, 91-97, <https://doi.org/10.1016/j.jes.2020.03.005>, 2020.

Liu, C., Hou, L., Liu, M., Zheng, Y., Yin, G., Han, P., Dong, H., Gao, J., Gao, D., Chang, Y., and Zhang, Z.: Coupling of denitrification and anaerobic ammonium oxidation with nitrification in sediments of the Yangtze Estuary: Importance and controlling factors, *Estuarine, Coastal Shelf Sci.*, 220, 64-72, <https://doi.org/10.1016/j.ecss.2019.02.043>, 2019.

Magri, M., Benelli, S., Bonaglia, S., Zilius, M., Castaldelli, G., and Bartoli, M.: The effects of hydrological extremes on denitrification, dissimilatory nitrate reduction to ammonium (DNRA) and mineralization in a coastal lagoon, *Sci. Total Environ.*, 740,

756 140169, <https://doi.org/10.1016/j.scitotenv.2020.140169>, 2020.

757 McTigue, N. D., Gardner, W. S., Dunton, K. H., and Hardison, A. K.: Biotic and
 758 abiotic controls on co-occurring nitrogen cycling processes in shallow Arctic shelf
 759 sediments, Nat. Commun., 7, 13145, <https://doi.org/10.1038/ncomms13145>, 2016.

760 Meyer, R. L., Risgaard-Petersen, N., and Allen, D. E.: Correlation between Anammox
 761 Activity and Microscale Distribution of Nitrite in a Subtropical Mangrove Sediment,
 762 Appl. Environ. Microbiol., 71, 6142-6149,
 763 <https://doi.org/10.1128/AEM.71.10.6142-6149.2005>, 2005.

764 [Middelburg, J. J., Soetaert, K., Herman, P. M. J., and Heip, C. H. R.: Denitrification in](#)
 765 [marine sediments: A model study, Global Biogeochem. Cycles, 10, 661-673,](#)
 766 <https://doi.org/10.1029/96GB02562>, 1996.

767 Na, T., Thamdrup, B., Kim, B., Kim, S.-H., Vandieken, V., Kang, D.-J., and Hyun,
 768 J.-H.: N₂ production through denitrification and anammox across the continental
 769 margin (shelf–slope–rise) of the Ulleung Basin, East Sea, Limnol. Oceanogr., 63,
 770 S410-S424, <https://doi.org/10.1002/lno.10750>, 2018.

771 Neubacher, E. C., Parker, R. E., and Trimmer, M.: Short-term hypoxia alters the
 772 balance of the nitrogen cycle in coastal sediments, Limnol. Oceanogr., 56, 651-665,
 773 <https://doi.org/10.4319/lo.2011.56.2.0651>, 2011.

774 Nielsen, L. P. and Glud, R. N.: Denitrification in a coastal sediment measured in situ
 775 by the nitrogen isotope pairing technique applied to a benthic flux chamber, Mar.
 776 Ecol.: Prog. Ser., 137, 181-186, <https://doi.org/10.3354/meps137181>, 1996.

777 Nielsen, L. P.: Denitrification in sediment determined from nitrogen isotope pairing,
 778 FEMS Microbiol. Lett., 86, 357-362, [https://doi.org/10.1016/0378-1097\(92\)90800-4](https://doi.org/10.1016/0378-1097(92)90800-4),
 779 1992.

780 Poulin, P., Pelletier, E., and Saint-Louis, R.: Seasonal variability of denitrification
 781 efficiency in northern salt marshes: An example from the St. Lawrence Estuary, Mar.
 782 Environ. Res., 63, 490-505, <https://doi.org/10.1016/j.marenvres.2006.12.003>, 2007.

783 Richardson, K., Steffen, W., Lucht, W., Bendtsen, J., Cornell, S. E., Donges, J. F.,
 784 Drüke, M., Fetzer, I., Bala, G., von Bloh, W., Feulner, G., Fiedler, S., Gerten, D.,
 785 Gleeson, T., Hofmann, M., Huiskamp, W., Kummu, M., Mohan, C., Nogués-Bravo,
 786 D., Petri, S., Porkka, M., Rahmstorf, S., Schaphoff, S., Thonicke, K., Tobian, A.,
 787 Virkki, V., Wang-Erlandsson, L., Weber, L., and Rockström, J.: Earth beyond six of
 788 nine planetary boundaries, Sci. Adv., 9, eadh2458,
 789 <https://doi.org/10.1126/sciadv.adh2458>, 2023.

790 Rios-Del Toro, E. E., Valenzuela, E. I., López-Lozano, N. E., Cortés-Martínez, M. G.,
 791 Sánchez-Rodríguez, M. A., Calvario-Martínez, O., Sánchez-Carrillo, S., and
 792 Cervantes, F. J.: Anaerobic ammonium oxidation linked to sulfate and ferric iron
 793 reduction fuels nitrogen loss in marine sediments, Biodegradation, 29, 429-442,
 794 <https://doi.org/10.1007/s10532-018-9839-8>, 2018.

795 Risgaard-Petersen, N., Nielsen, L. P., Rysgaard, S., Dalsgaard, T., and Meyer, R. L.:
 796 Application of the isotope pairing technique in sediments where anammox and
 797 denitrification coexist, Limnol. Oceanogr.: Methods, 1, 63-73,
 798 <https://doi.org/10.4319/lom.2003.1.63>, 2003.

799 Risgaard-Petersen, N., Meyer, R. L., Schmid, M., Jetten, M., S. M. , Enrich-Prast, A.,
 800 Rysgaard, S., and Revsbech, N. P.: Anaerobic ammonium oxidation in an estuarine
 801 sediment, Aquat. Microb. Ecol., 36, 293-304, <https://doi.org/10.3354/ame036293>,
 802 2004.

803 Robertson, E. K., Bartoli, M., Brüchert, V., Dalsgaard, T., Hall, P. O. J., Hellemann,
 804 D., Hietanen, S., Zilius, M., and Conley, D. J.: Application of the isotope pairing
 805 technique in sediments: Use, challenges, and new directions, Limnol. Oceanogr.:

806 Methods, 17, 112-136, <https://doi.org/10.1002/lom3.10303>, 2019.

807 Rosales Villa, A. R., Jickells, T. D., Sivy, D. B., Parker, E. R., and Thamdrup, B.:
808 Benthic nitrogen cycling in the North Sea, Cont. Shelf Res., 185, 31-36,
809 <https://doi.org/10.1016/j.csr.2018.05.005>, 2019.

810 Rysgaard, S., Finster, K., and Dahlgaard, H.: Primary production, nutrient dynamics
811 and mineralisation in a northeastern Greenland fjord during the summer thaw, Polar
812 Biology, 16, 497-506, <https://doi.org/10.1007/BF02329069>, 1996a.

813 Rysgaard, S., Fossing, H., and Jensen, M. M.: Organic matter degradation through
814 oxygen respiration, denitrification, and manganese, iron, and sulfate reduction in
815 marine sediments (the Kattegat and the Skagerrak), Ophelia, 55, 77-91,
816 <https://doi.org/10.1080/00785236.2001.10409475>, 2001.

817 Rysgaard, S., Risgaard-Petersen, N., and Sloth, N. P.: Nitrification, denitrification, and
818 nitrate ammonification in sediments of two coastal lagoons in Southern France,
819 Hydrobiologia, 329, 133-141, <https://doi.org/10.1007/BF00034553>, 1996b.

820 Rysgaard, S., Glud, R. N., Risgaard-Petersen, N., and Dalsgaard, T.: Denitrification
821 and anammox activity in Arctic marine sediments, Limnol. Oceanogr., 49, 1493-1502,
822 <https://doi.org/10.4319/lo.2004.49.5.1493>, 2004.

823 Salk, K. R., Erler, D. V., Eyre, B. D., Carlson-Perret, N., and Ostrom, N. E.:
824 Unexpectedly high degree of anammox and DNRA in seagrass sediments: Description
825 and application of a revised isotope pairing technique, Geochim. Cosmochim. Acta,
826 211, 64-78, <https://doi.org/10.1016/j.gca.2017.05.012>, 2017.

827 Samperio-Ramos, G., Hernández-Sánchez, O., Camacho-Ibar, V. F., Pajares, S.,
828 Gutiérrez, A., Sandoval-Gil, J. M., Reyes, M., De Gyves, S., Balint, S., Oczkowski, A.,
829 Ponce-Jahen, S. J., and Cervantes, F. J.: Ammonium loss microbiologically mediated
830 by Fe(III) and Mn(IV) reduction along a coastal lagoon system, Chemosphere, 349,

831 [140933, https://doi.org/10.1016/j.chemosphere.2023.140933](https://doi.org/10.1016/j.chemosphere.2023.140933), 2024.

832 Sokoll, S., Holtappels, M., Lam, P., Collins, G., Schlüter, M., Lavik, G., and Kuypers,
833 M.: Benthic Nitrogen Loss in the Arabian Sea Off Pakistan, *Front. Microbiol.*, 3,
834 <https://doi.org/10.3389/fmicb.2012.00395>, 2012.

835 Song, G., Liu, S., Zhu, Z., Zhai, W., Zhu, C., and Zhang, J.: Sediment oxygen
836 consumption and benthic organic carbon mineralization on the continental shelves of
837 the East China Sea and the Yellow Sea, *Deep Sea Res., Part II.*, 124, 53-63,
838 <https://doi.org/10.1016/j.dsr2.2015.04.012>, 2016a.

839 Song, G., Liu, S., Zhang, J., Zhu, Z., Zhang, G., Marchant, H. K., Kuypers, M. M. M.,
840 and Lavik, G.: Response of benthic nitrogen cycling to estuarine hypoxia, *Limnol.*
841 *Oceanogr.*, 66, 652-666, <https://doi.org/10.1002/lno.11630>, 2021.

842 Song, G. D., Liu, S. M., Kuypers, M. M. M., and Lavik, G.: Application of the isotope
843 pairing technique in sediments where anammox, denitrification, and dissimilatory
844 nitrate reduction to ammonium coexist, *Limnol. Oceanogr.: Methods*, 14, 801-815,
845 <https://doi.org/10.1002/lom3.10127>, 2016b.

846 Steingruber, S. M., Friedrich, J., Gächter, R., and Wehrli, B.: Measurement of
847 Denitrification in Sediments with the ¹⁵N Isotope Pairing Technique, *Appl. Environ.*
848 *Microbiol.*, 67, 3771-3778, <https://doi.org/10.1128/AEM.67.9.3771-3778.2001>, 2001.

849 Strous, M., Fuerst, J. A., Kramer, E. H. M., Logemann, S., Muyzer, G., van de
850 Pas-Schoonen, K. T., Webb, R., Kuenen, J. G., and Jetten, M. S. M.: Missing
851 lithotroph identified as new planctomycete, *Nature*, 400, 446-449,
852 <https://doi.org/10.1038/22749>, 1999.

853 Susanna, H.: Anaerobic ammonium oxidation (anammox) in sediments of the Gulf of
854 Finland, *Aquat. Microb. Ecol.*, 48, 197-205, <https://doi.org/10.3354/ame048197>,
855 2007.

删除[小子]: Shan, J., Zhao, X., Sheng, R., Xia, Y., ti, C.,
Quan, X., Wang, S., Wei, W., and Yan, X.: Dissimilatory
Nitrate Reduction Processes in Typical Chinese Paddy Soils:
Rates, Relative Contributions, and Influencing Factors,
Environ. Sci. Technol., 50, 9972-9980,
<https://doi.org/10.1021/acs.est.6b01765>, 2016.

856 Tan, E., Zou, W., Jiang, X., Wan, X., Hsu, T.-C., Zheng, Z., Chen, L., Xu, M., Dai, M.,
857 and Kao, S.-j.: Organic matter decomposition sustains sedimentary nitrogen loss in
858 the Pearl River Estuary, China, *Sci. Total Environ.*, 648, 508-517,
859 <https://doi.org/10.1016/j.scitotenv.2018.08.109>, 2019.

860 Tan, E., Zou, W., Zheng, Z., Yan, X., Du, M., Hsu, T.-C., Tian, L., Middelburg, J. J.,
861 Trull, T. W., and Kao, S.-j.: Warming stimulates sediment denitrification at the
862 expense of anaerobic ammonium oxidation, *Nat. Clim. Change*, 10, 349-355,
863 <https://doi.org/10.1038/s41558-020-0723-2>, 2020.

864 Tan, E., Hsu, T.-C., Zou, W., Yan, X., Huang, Z., Chen, B., Chang, Y., Zheng, Z.,
865 Zheng, L., Xu, M., Tian, L., and Kao, S.-J.: Quantitatively deciphering the roles of
866 sediment nitrogen removal in environmental and climatic feedbacks in two
867 subtropical estuaries, *Water Res.*, 224, 119121,
868 <https://doi.org/10.1016/j.watres.2022.119121>, 2022.

869 Thamdrup, B.: New Pathways and Processes in the Global Nitrogen Cycle, *Annu. Rev.*
870 *Ecol. Evol. Syst.*, 43, 407-428,
871 <https://doi.org/10.1146/annurev-ecolsys-102710-145048>, 2012.

872 Thamdrup, B. and Dalsgaard, T.: Production of N₂ through Anaerobic Ammonium
873 Oxidation Coupled to Nitrate Reduction in Marine Sediments, *Appl. Environ.*
874 *Microbiol.*, 68, 1312-1318, <https://doi.org/10.1128/AEM.68.3.1312-1318.2002>, 2002.

875 Torregrosa-Crespo, J., Miralles-Robledillo, J. M., Bernabeu, E., Pire, C., and
876 Martínez-Espinosa, R. M.: Denitrification in hypersaline and coastal environments,
877 *FEMS Microbiol. Lett.*, 370, <https://doi.org/10.1093/femsle/fnad066>, 2023.

878 Trimmer, M. and Nicholls, J. C.: Production of nitrogen gas via anammox and
879 denitrification in intact sediment cores along a continental shelf to slope transect in
880 the North Atlantic, *Limnol. Oceanogr.*, 54, 577-589,
881 <https://doi.org/10.4319/lo.2009.54.2.0577>, 2009.

882 Trimmer, M., Engström, P., and Thamdrup, B.: Stark Contrast in Denitrification and
883 Anammox across the Deep Norwegian Trench in the Skagerrak, Appl. Environ.
884 Microbiol., 79, 7381-7389, <https://doi.org/10.1128/AEM.01970-13>, 2013.

885 Trimmer, M., Nicholls, J. C., and Deflandre, B.: Anaerobic Ammonium Oxidation
886 Measured in Sediments along the Thames Estuary, United Kingdom, Appl. Environ.
887 Microbiol., 69, 6447-6454, <https://doi.org/10.1128/AEM.69.11.6447-6454.2003>,
888 2003.

889 Trimmer, M., Risgaard-Petersen, N., Nicholls, J. C., and Engström, P.: Direct
890 measurement of anaerobic ammonium oxidation (anammox) and denitrification in
891 intact sediment cores, Mar. Ecol.: Prog. Ser., 326, 37-47,
892 <https://doi.org/10.3354/meps326037>, 2006.

893 Usui, T., Koike, I., and Ogura, N.: N₂O Production, Nitrification and Denitrification in
894 an Estuarine Sediment, Estuarine, Coastal Shelf Sci., 52, 769-781,
895 <https://doi.org/10.1006/ecss.2000.0765>, 2001.

896 Uusheimo, S., Huotari, J., Tulonen, T., Aalto, S. L., Rissanen, A. J., and Arvola, L.:
897 High Nitrogen Removal in a Constructed Wetland Receiving Treated Wastewater in a
898 Cold Climate, Environ. Sci. Technol., 52, 13343-13350,
899 <https://doi.org/10.1021/acs.est.8b03032>, 2018.

900 Vance-Harris, C. and Ingall, E.: Denitrification pathways and rates in the sandy
901 sediments of the Georgia continental shelf, USA, Geochem. Trans., 6, 12,
902 <https://doi.org/10.1186/1467-4866-6-12>, 2005.

903 Wan, R., Ge, L., Chen, B., Tang, J.-M., Tan, E., Zou, W., Tian, L., Li, M., Liu, Z., Hou,
904 L., Yin, G., and Kao, S.-J.: Permeability decides the effect of antibiotics on
905 sedimentary nitrogen removal in Jiulong River Estuary, Water Res., 243, 120400,
906 <https://doi.org/10.1016/j.watres.2023.120400>, 2023.

907 Welsh, D. T., Bartoli, M., Nizzoli, D., Castaldelli, G., Riou, S. A., and Viaroli, P.:
 908 Denitrification, nitrogen fixation, community primary productivity and inorganic-N
 909 and oxygen fluxes in an intertidal *Zostera noltii* meadow, Mar. Ecol.: Prog. Ser., 208,
 910 65-77, <https://doi.org/10.3354/meps208065>, 2000.

911 Yang, J.-Y. T., Hsu, T.-C., Tan, E., Lee, K., Krom, M. D., Kang, S., Dai, M., Hsiao, S.
 912 S.-Y., Yan, X., Zou, W., Tian, L., and Kao, S.-J.: Sedimentary processes dominate
 913 nitrous oxide production and emission in the hypoxic zone off the Changjiang River
 914 estuary, Sci. Total Environ., 827, 154042,
 915 <https://doi.org/10.1016/j.scitotenv.2022.154042>, 2022.

916 Yin, G., Hou, L., Zong, H., Ding, P., Liu, M., Zhang, S., Cheng, X., and Zhou, J.:
 917 Denitrification and Anaerobic Ammonium Oxidization Across the Sediment–Water
 918 Interface in the Hypereutrophic Ecosystem, Jinpu Bay, in the Northeastern Coast of
 919 China, Estuaries Coasts, 38, 211-219, <https://doi.org/10.1007/s12237-014-9798-1>,
 920 2015.

921

Figures and Table

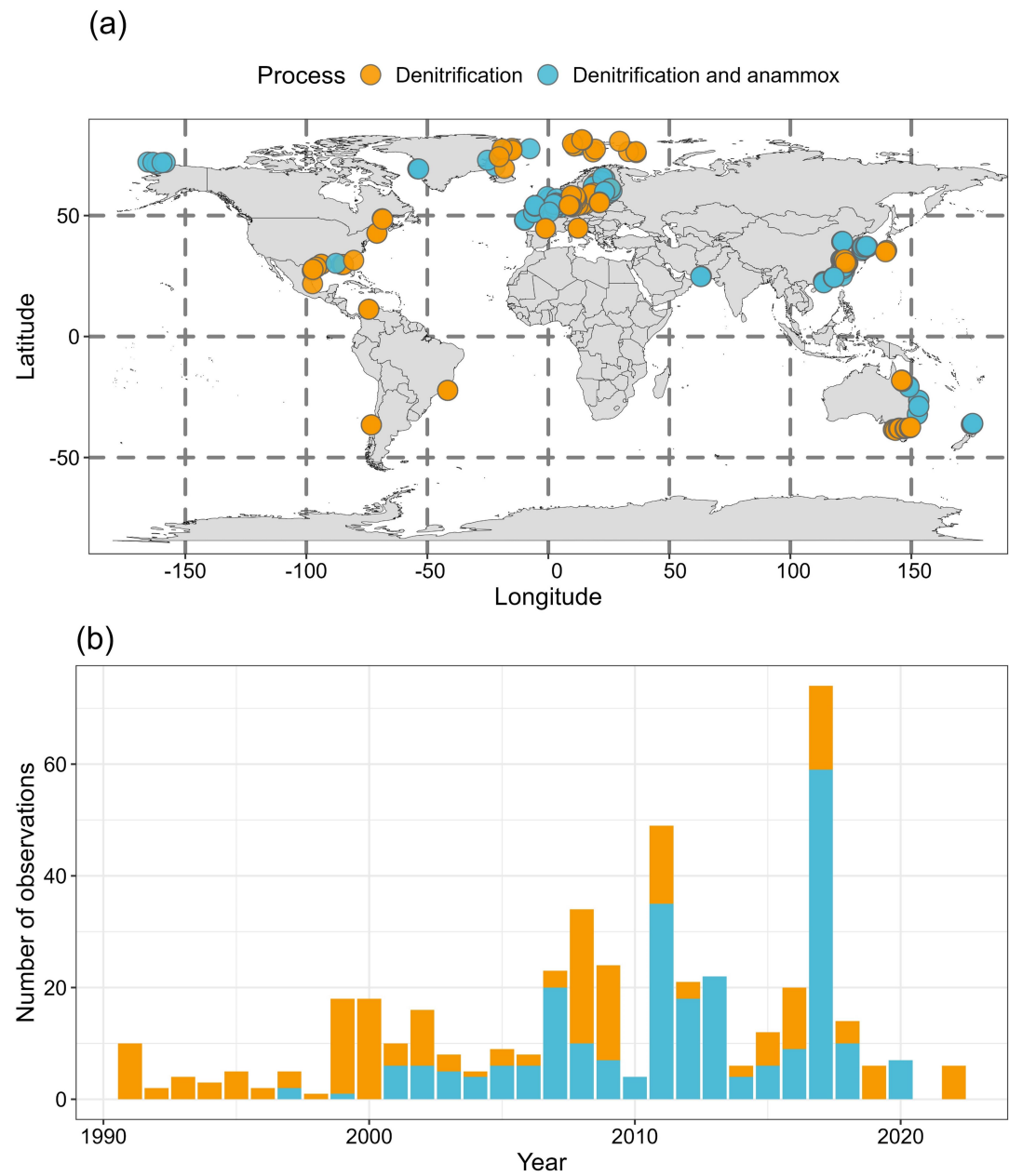


Figure 1 Map showing the sampling sites distribution of nitrogen loss rate measurements (a) and the number of rate observations each year (b). Orange solid points denote that only denitrification rates were measured. Cyan solid points denote that both denitrification and anammox rates were measured.

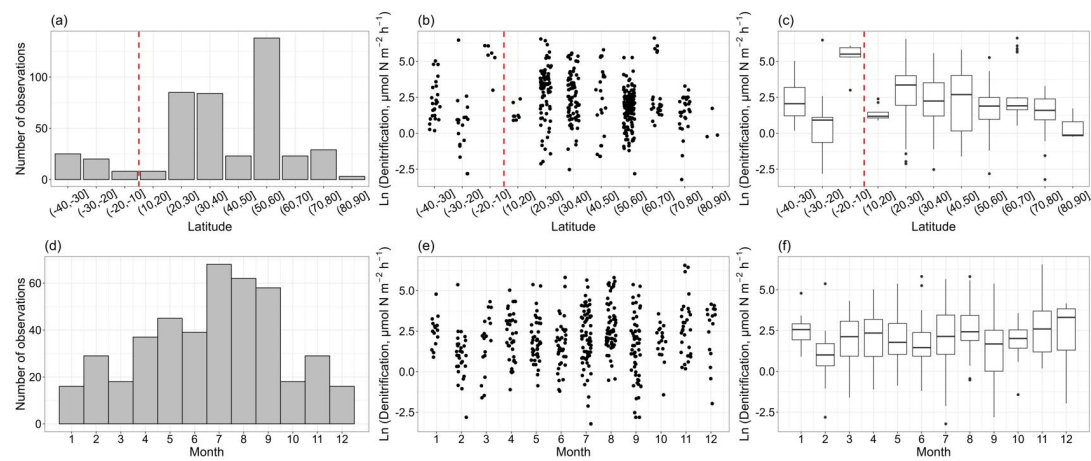


Figure 2 The observation numbers of denitrification (a, d) and denitrification rates (b, c, e, f) with latitudinal bands and months. A vertical dashed red line delimits the Southern Hemisphere and the Northern Hemisphere. The box plots show the median, interquartile range, and outliers for each latitudinal band and month.

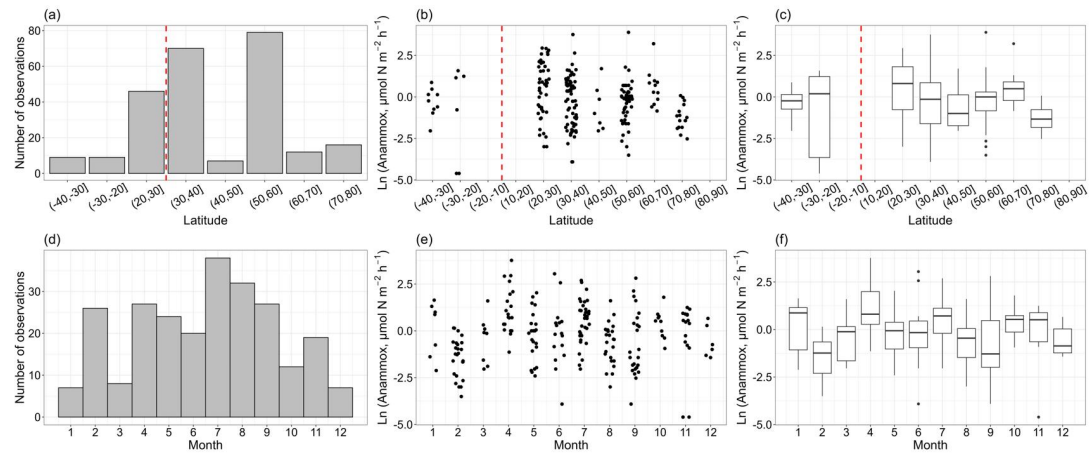
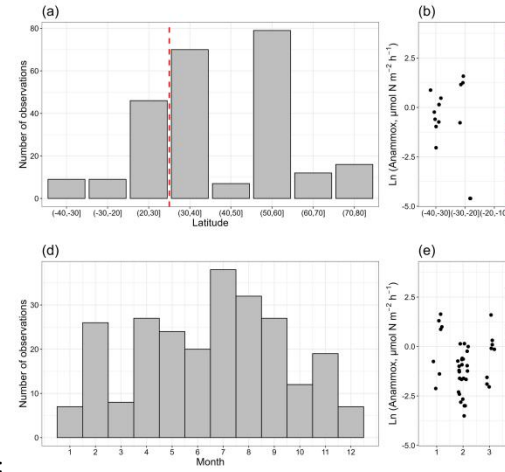


Figure 3 The observation numbers of anammox (a, d) and anammox rates (b, c, e, f) with latitudinal bands and months.

删除[小子]:

设置格式[小子]: 字体: (默认)Times New Roman, 小四, 字体颜色: 自动设置

删除[小子]: Tops and bottoms of boxes in box plots denote the 25th and 75th percentiles, respectively. The horizontal lines inside the box plots represent the medians. Whiskers mark the minimum and maximum values within 1.5 times the interquartile range, with black points representing outliers beyond that range.



删除[小子]:

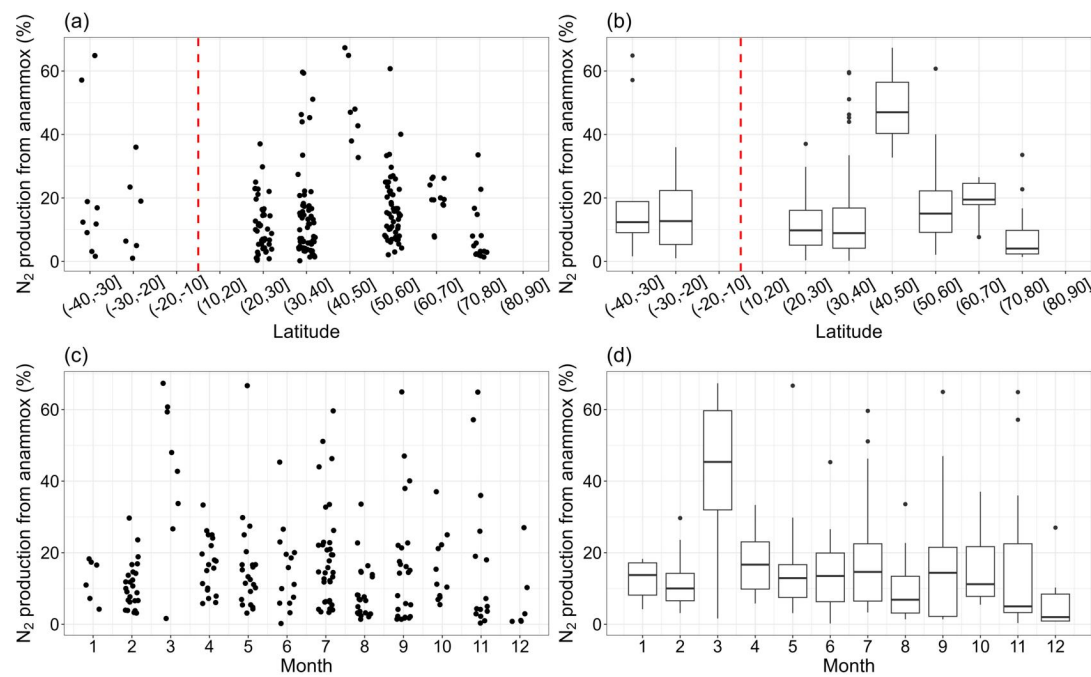
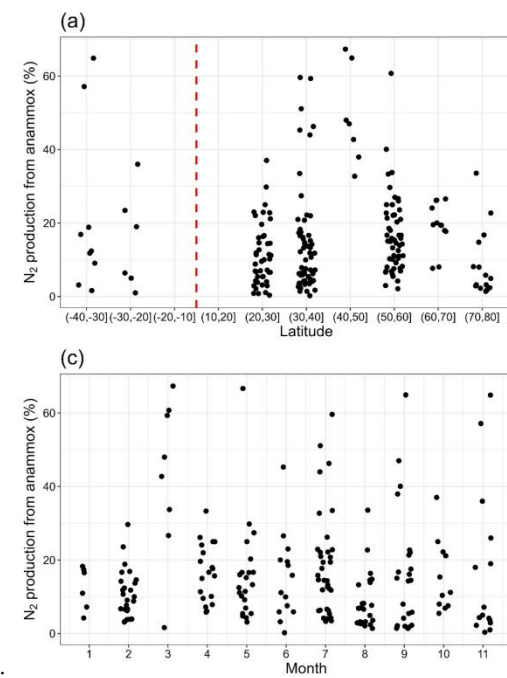


Figure 4 The contribution of anammox to total N_2 production with latitudinal bands (a, b) and months (c, d).



删除[小子]:

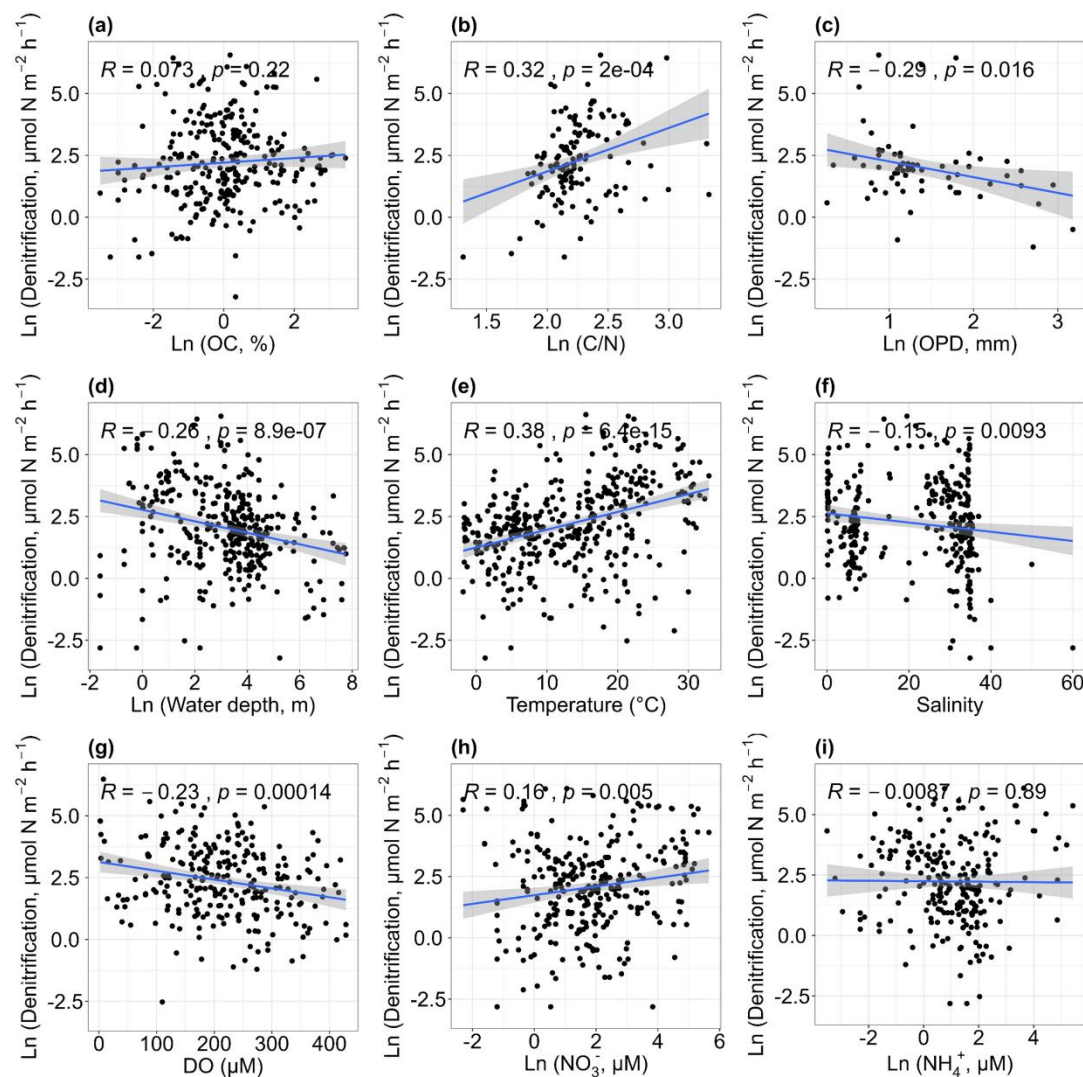


Figure 5 Relationships between denitrification rates and organic carbon [OC, (a)], carbon-nitrogen ratios [C/N, (b)], oxygen penetration depth [OPD, (c)], water depth (d), temperature (e), salinity (f), dissolved oxygen [DO, (g)], nitrate concentrations [NO_3^- , (h)] and ammonium concentrations [NH_4^+ , (i)].

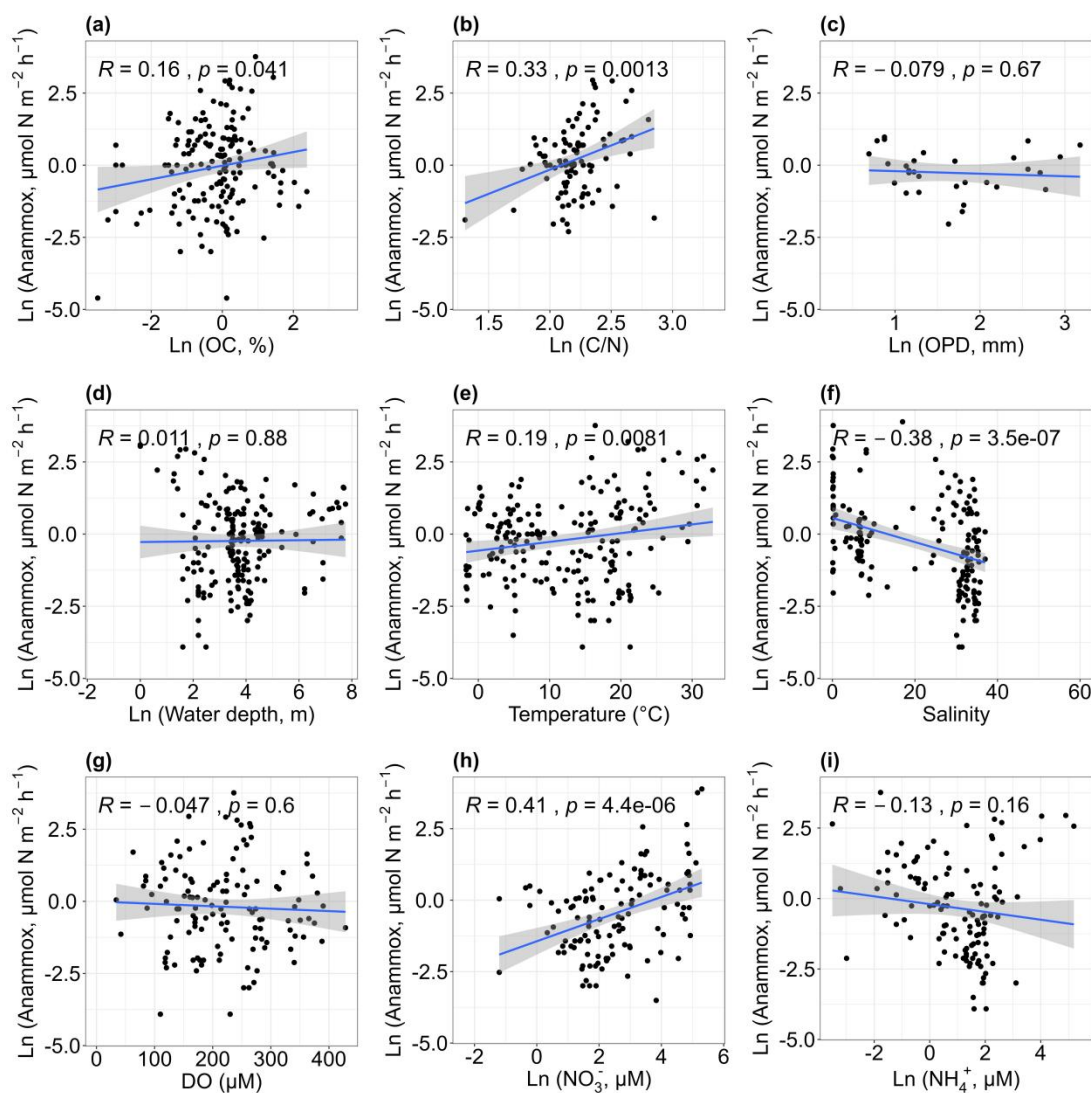
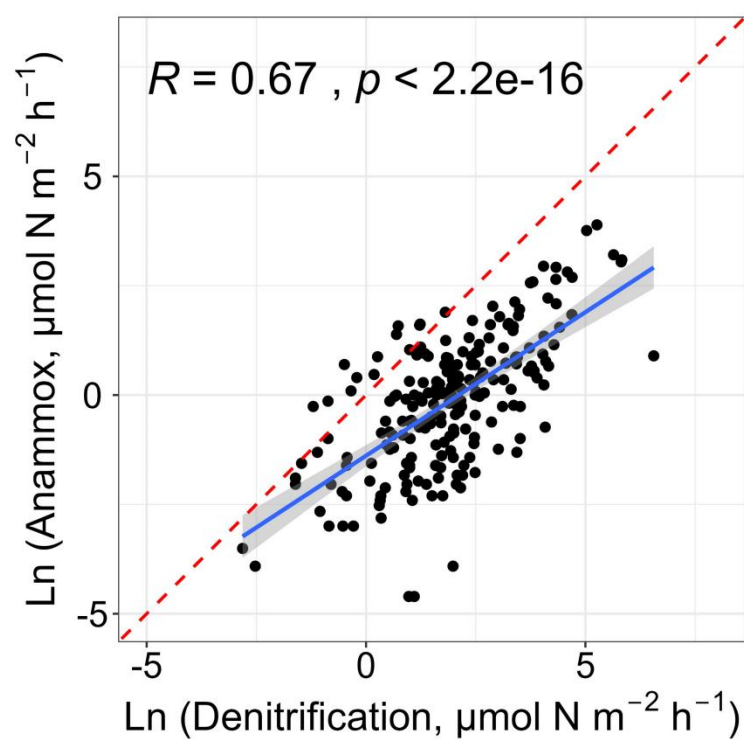


Figure 6 Relationships between anammox rates and organic carbon [OC, (a)], carbon-nitrogen ratios [C/N, (b)], oxygen penetration depth [OPD, (c)], water depth (d), temperature (e), salinity (f), dissolved oxygen [DO, (g)], nitrate concentrations [NO₃⁻, (h)] and ammonium concentrations [NH₄⁺, (i)].



956

957 **Figure 7** Relationships between denitrification and anammox rates. The blue solid
 958 line and red dashed line denote the linear regression and 1:1 line, respectively.

959

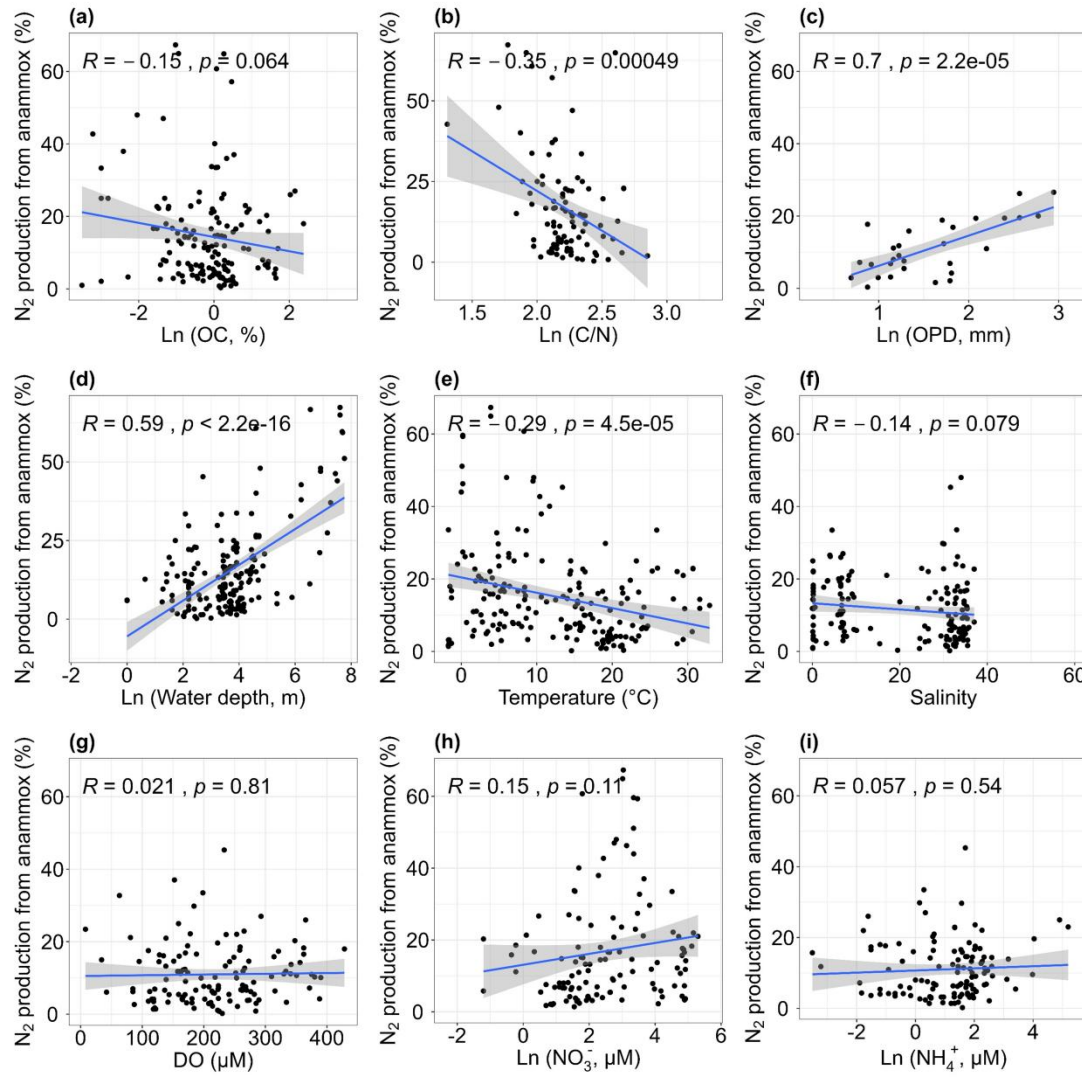


Figure 8 Relationships between the relative contribution of anammox to total N_2 production and organic carbon [OC, (a)], carbon-nitrogen ratios [C/N, (b)], oxygen penetration depth [OPD, (c)], water depth (d), temperature (e), salinity (f), dissolved oxygen [DO, (g)], nitrate concentrations [NO_3^- , (h)] and ammonium concentrations [NH_4^+ , (i)].

966 **Table 1** Summary of the observations of actual nitrogen loss rates. The locations,
967 water depth range, observation numbers, core incubation methods and references are
968 listed.

<u>Sampling locations</u>	<u>Water depth (m)</u>	<u>Observation numbers</u>	<u>Core incubations</u>	<u>References</u>
<u>Aarhus Bright, Denmark</u>	<u>16</u>	<u>2</u>	<u>Intact core incubations</u>	<u>(Nielsen and Glud, 1996)</u>
<u>Arabian Sea</u>	<u>360 - 1430</u>	<u>4</u>	<u>Intact core incubations</u>	<u>(Sokoll et al., 2012)</u>
<u>Arctic fjord (Svalbard, Norway)</u>	<u>51 - 211</u>	<u>3</u>	<u>Intact core incubations</u>	<u>(Gihring et al., 2010b)</u>
<u>Bassin d’Arcachon coastal lagoon</u>	<u>NM</u>	<u>3</u>	<u>Intact core incubations</u>	<u>(Welsh et al., 2000)</u>
<u>Casino, NSW, Australia</u>	<u>NM</u>	<u>2</u>	<u>Intact core incubations</u>	<u>(Erler et al., 2008)</u>
<u>central Sagami Bay, Japan</u>	<u>25.1 - 59</u>	<u>1</u>	<u>Intact core incubations</u>	<u>(Glud et al., 2009)</u>
<u>Changjiang estuary and its adjacent East China Sea</u>	<u>1.9 - 58</u>	<u>7</u>	<u>Intact core incubations</u>	<u>(Song et al., 2021)</u>
<u>Changjiang River Estuary and Jiulong River Estuary, China</u>	<u>NM</u>	<u>23</u>	<u>Intact core incubations</u>	<u>(Tan et al., 2022)</u>
<u>Changjiang River Estuary, China</u>	<u>6 - 61</u>	<u>22</u>	<u>Continuous- flow experiments</u>	<u>(Liu et al., 2020)</u>
<u>Changjiang River Estuary, China</u>	<u>24 - 33</u>	<u>14</u>	<u>Continuous- flow experiments</u>	<u>(Liu et al., 2019)</u>
<u>Coast of Finland, northern Baltic Sea</u>	<u>1.5 - 8</u>	<u>10</u>	<u>Intact core incubations</u>	<u>(Hellemann et al., 2020)</u>
<u>Coast of Victoria, Australia</u>	<u>5 - 24</u>	<u>11</u>	<u>Intact core incubations</u>	<u>(Kessler et al., 2018)</u>
<u>Coastal area of the Gulf of Gdańsk</u>	<u>NM</u>	<u>6</u>	<u>Intact core incubations</u>	<u>(Benelli et al., 2024)</u>
<u>Coastal lagoons, France</u>	<u>36 - 100</u>	<u>6</u>	<u>Intact core incubations</u>	<u>(Rysgaard et al., 1996b)</u>
<u>Coastal sediments, Greenland</u>	<u>50 - 2000</u>	<u>11</u>	<u>Intact core incubations</u>	<u>(Rysgaard et al., 2004)</u>
<u>Continental shelf and slope, North Atlantic</u>	<u>85</u>	<u>12</u>	<u>Intact core incubations</u>	<u>(Trimmer and Nicholls, 2009)</u>
<u>Continental shelf region off central Chile</u>	<u>NM</u>	<u>5</u>	<u>Intact core incubations</u>	<u>(Farias et al., 2004)</u>
<u>Danshuei River in northern</u>	<u>19 - 43.5</u>	<u>1</u>	<u>Intact core</u>	<u>(Hsu and Kao,</u>

删除[小子]: Sampling locations

Observation numbers

Core incubations

References

Aarhus Bright, Denmark

2

Intact core incubations

(Nielsen and Glud, 1996)

Arabian Sea

4

Intact core incubations

(Sokoll et al., 2012)

Arctic fjord (Svalbard, Norway)

3

Intact core incubations

(Gihring et al., 2010b)

Bassin d’Arcachon coastal lagoon

3

Intact core incubations

(Welsh et al., 2000)

Casino, NSW, Australia

2

Intact core incubations

(Erler et al., 2008)

central Sagami Bay, Japan

1

Intact core incubations

(Glud et al., 2009)

Changjiang estuary and its adjacent East China Sea

7

Intact core incubations

(Song et al., 2021)

Changjiang River Estuary and Jiulong River Estuary, China

23

Intact core incubations

(Tan et al., 2022)

Changjiang River Estuary, China

22

Continuous-flow experiments

(Liu et al., 2020)

Changjiang River Estuary, China

14

Continuous-flow experiments

<u>Taiwan, China</u>			<u>incubations</u>	<u>2013)</u>
<u>East China Sea</u>	<u>0.7 - 7.9</u>	<u>2</u>	<u>Intact core</u>	<u>(Song et al.,</u>
			<u>incubations</u>	<u>2016)</u>
<u>Elbe Estuary, North Frisian</u>	<u>115 - 329</u>	<u>5</u>	<u>Intact core</u>	<u>(Deek et al.,</u>
<u>Wadden Sea</u>			<u>incubations</u>	<u>2013)</u>
<u>Fjords in Svalbard and</u>	<u>27 - 40</u>	<u>5</u>	<u>Intact core</u>	<u>(Glud et al.,</u>
<u>northern Norway</u>			<u>incubations</u>	<u>1998)</u>
<u>Georgia continental shelf,</u>	<u>5 - 29</u>	<u>2</u>	<u>Intact core</u>	<u>(Vance-Harris</u>
<u>USA</u>			<u>incubations</u>	<u>and Ingall,</u>
				<u>2005)</u>
<u>Great Barrier Reef lagoon</u>	<u>12.5 - 111</u>	<u>2</u>	<u>Intact core</u>	<u>(Erler et al.,</u>
			<u>incubations</u>	<u>2013)</u>
<u>Gulf of Bothnia, Baltic Sea</u>	<u>13 - 85</u>	<u>7</u>	<u>Intact core</u>	<u>(Bonaglia et</u>
			<u>incubations</u>	<u>al., 2017)</u>
<u>Gulf of Finland</u>	<u>58 - 83</u>	<u>5</u>	<u>Intact core</u>	<u>(Susanna,</u>
			<u>incubations</u>	<u>2007)</u>
				<u>(Jäntti and</u>
<u>Gulf of Finland, Baltic Sea</u>	<u>NM</u>	<u>11</u>	<u>Intact core</u>	<u>Hietanen,</u>
			<u>incubations</u>	<u>2012)</u>
<u>Gulf of Finland, Baltic Sea</u>	<u>33</u>	<u>13</u>	<u>Intact core</u>	<u>(Jäntti et al.,</u>
			<u>incubations</u>	<u>2011)</u>
				<u>(Hietanen and</u>
<u>Gulf of Finland, Baltic Sea</u>	<u>NM</u>	<u>5</u>	<u>Intact core</u>	<u>Kuparinen,</u>
			<u>incubations</u>	<u>2008)</u>
<u>Gulf of Mexico</u>	<u>116</u>	<u>6</u>	<u>Intact core</u>	<u>(Gihring et</u>
			<u>incubations</u>	<u>al., 2010a)</u>
<u>Gullmarsfjorden, Sweden and</u>	<u>12 - 63</u>	<u>2</u>	<u>Intact core</u>	<u>(Trimmer et</u>
<u>Thames Estuary, England</u>			<u>incubations</u>	<u>al., 2006)</u>
<u>Hypoxic zone off the</u>				
<u>Changjiang River estuary,</u>	<u>5 - 15</u>	<u>9</u>	<u>Intact core</u>	<u>(Yang et al.,</u>
<u>China</u>			<u>incubations</u>	<u>2022)</u>
			<u>Continuous-</u>	
<u>Jinpu Bay, China</u>	<u>4.1 - 11.8</u>	<u>12</u>	<u>flow</u>	<u>(Yin et al.,</u>
			<u>experiments</u>	<u>2015)</u>
<u>Jiulong River Estuary, China</u>	<u>10 - 695</u>	<u>2</u>	<u>Intact core</u>	<u>(Wan et al.,</u>
			<u>incubations</u>	<u>2023)</u>
<u>Kattegat and Skagerrak</u>	<u>345</u>	<u>10</u>	<u>Intact core</u>	<u>(Rysgaard et</u>
			<u>incubations</u>	<u>al., 2001)</u>
<u>Lawrence estuary</u>	<u>1.5</u>	<u>1</u>	<u>Intact core</u>	<u>(Crowe et al.,</u>
			<u>incubations</u>	<u>2012)</u>
			<u>Continuous-</u>	
<u>Little Lagoon, USA</u>	<u>NM</u>	<u>1</u>	<u>flow</u>	<u>(Bernard et</u>
			<u>experiments</u>	<u>al., 2015)</u>
<u>Noosa River estuary,</u>	<u>0 - 116</u>	<u>5</u>	<u>Intact core</u>	<u>(Chen et al.,</u>

<u>Australia</u>			<u>incubations</u>	<u>2021)</u>
<u>North Sea</u>	<u>31</u>	<u>9</u>	<u>Intact core</u>	<u>(Rosales Villa</u>
			<u>incubations</u>	<u>et al., 2019)</u>
<u>North Sea</u>	<u>9 - 49</u>	<u>1</u>	<u>Intact core</u>	<u>(Fan et al.,</u>
			<u>incubations</u>	<u>2015)</u>
<u>North Sea</u>	<u>29 - 81</u>	<u>8</u>	<u>Intact core</u>	<u>(Bale et al.,</u>
			<u>incubations</u>	<u>2014)</u>
<u>North Sea</u>	<u>41 - 66</u>	<u>16</u>	<u>Intact core</u>	<u>(Neubacher et</u>
			<u>incubations</u>	<u>al., 2011)</u>
<u>Northeast Chukchi Sea</u>	<u>30 - 128</u>	<u>5</u>	<u>Continuous-</u>	<u>(McTigue et</u>
			<u>flow</u>	<u>al., 2016)</u>
			<u>experiments</u>	
<u>Northeastern New Zealand</u>	<u>31 - 41</u>	<u>7</u>	<u>Intact core</u>	<u>(Cheung et</u>
<u>continental shelf</u>			<u>incubations</u>	<u>al., 2024)</u>
<u>Northern Baltic Proper</u>	<u>27.7 - 64.8</u>	<u>17</u>	<u>Intact core</u>	<u>(Bonaglia et</u>
			<u>incubations</u>	<u>al., 2014a)</u>
<u>Northern East China Sea,</u>	<u>176 - 688</u>	<u>16</u>	<u>Continuous-</u>	<u>(Chang et al.,</u>
<u>China</u>			<u>flow</u>	<u>2021)</u>
			<u>experiments</u>	
<u>Norwegian Trench, Skagerrak</u>	<u>NM</u>	<u>4</u>	<u>Intact core</u>	<u>(Trimmer et</u>
			<u>incubations</u>	<u>al., 2013)</u>
<u>Öre Estuary, Swedish</u>	<u>7-26</u>	<u>6</u>	<u>Intact core</u>	<u>(Hellemann et</u>
			<u>incubations</u>	<u>al., 2017)</u>
<u>Pearl River Estuary, China</u>	<u>NM</u>	<u>5</u>	<u>Intact core</u>	<u>(Tan et al.,</u>
			<u>incubations</u>	<u>2019)</u>
<u>Plum Island Sound,</u>	<u>0.5 - 1</u>	<u>4</u>	<u>Intact core</u>	<u>(Koop-Jakobs</u>
<u>Massachusetts</u>			<u>incubations</u>	<u>en and Giblin,</u>
				<u>2010)</u>
<u>Randers Fjord and Norsminde</u>	<u>1 - 695</u>	<u>2</u>	<u>Intact core</u>	<u>(Risgaard-Pet</u>
<u>Fjord, Denmark</u>			<u>incubations</u>	<u>ersen et al.,</u>
				<u>2004)</u>
<u>Randers Fjord, Young Sound</u>	<u>NM</u>	<u>3</u>	<u>Intact core</u>	<u>(Risgaard-Pet</u>
<u>and Skagerrak, Danmark</u>			<u>incubations</u>	<u>ersen et al.,</u>
				<u>2003)</u>
<u>Sacca di Goro lagoon, Italy</u>	<u>1450</u>	<u>6</u>	<u>Intact core</u>	<u>(Magri et al.,</u>
			<u>incubations</u>	<u>2020)</u>
<u>Southern and central Baltic</u>	<u>0.2 - 80</u>	<u>12</u>	<u>Intact core</u>	<u>(Deutsch et</u>
<u>Sea</u>			<u>incubations</u>	<u>al., 2010)</u>
<u>Southern Finland</u>	<u>NM</u>	<u>5</u>	<u>Intact core</u>	<u>(Uusheimo et</u>
			<u>incubations</u>	<u>al., 2018)</u>
<u>St. George Island, Gulf of</u>				
<u>Mexico, Hausstrand, German</u>	<u>NM</u>	<u>5</u>	<u>Intact core</u>	<u>(Canion et al.,</u>
<u>Wadden Sea and Spitsbergen</u>			<u>incubations</u>	<u>2014)</u>
<u>island, Svalbard</u>				

<u>St. Joseph Bay, USA</u>	<u>0.82</u>	<u>4</u>	<u>Continuous-flow experiments</u>	<u>(Hoffman et al., 2019)</u>
<u>St. Lawrence Estuary, Canada</u>	<u>NM</u>	<u>3</u>	<u>Intact core incubations</u>	<u>(Poulin et al., 2007)</u>
<u>Stockholm Archipelago, Baltic Sea</u>	<u>28</u>	<u>1</u>	<u>Intact core incubations</u>	<u>(Bonaglia et al., 2014b)</u>
<u>Svalbard, Norway</u>	<u>170 - 869</u>	<u>10</u>	<u>Intact core incubations</u>	<u>(Blackburn et al., 1996)</u>
<u>Taganga Bay, Colombia Caribbean</u>	<u>NM</u>	<u>8</u>	<u>Intact core incubations</u>	<u>(Arroyave Gómez et al., 2020)</u>
<u>Tama Estuary, Japan</u>	<u>20 - 30</u>	<u>2</u>	<u>Continuous-flow experiments</u>	<u>(Usui et al., 2001)</u>
<u>Texas estuaries, USA</u>	<u>0.6 - 3</u>	<u>26</u>	<u>Continuous-flow experiments</u>	<u>(Gardner et al., 2006)</u>
<u>The Baltic Sea</u>	<u>105</u>	<u>1</u>	<u>Intact core incubations</u>	<u>(Bonaglia et al., 2013)</u>
<u>The Curonian Lagoon</u>	<u>1 - 2.5</u>	<u>8</u>	<u>Intact core incubations</u>	<u>(Bartoli et al., 2021)</u>
<u>Tropical Coastal Lagoons</u>	<u>0.2 - 3</u>	<u>11</u>	<u>Intact core incubations</u>	<u>(Enrich-Prast et al., 2016a)</u>
<u>Tropical Coastal Wetlands, Australia</u>	<u>NM</u>	<u>8</u>	<u>Intact core incubations</u>	<u>(Adame et al., 2019b)</u>
<u>Ulleung Basin, East Sea</u>	<u>72 - 2342</u>	<u>9</u>	<u>Intact core incubations</u>	<u>(Na et al., 2018)</u>
<u>Wallis Lake estuary, Australia</u>	<u>NM</u>	<u>2</u>	<u>Intact core incubations</u>	<u>(Erler et al., 2017)</u>
<u>Young Sound fjord, northeast Greenland</u>	<u>40</u>	<u>1</u>	<u>Intact core incubations</u>	<u>(Rysgaard et al., 1996a)</u>

969

NM denotes that water depth is not mentioned,

删除[小子]: Continuous-flow experiments denote continuous flow experiments combined with core incubations